TO STUDY THE EFFICIENCY OF CR-39 BASED DOSIMETERS

A Dissertation Submitted to the Quaid-i-Azam University in Partial Fulfillment of the Requirement for the Degree of

Master of Philosophy

in

Physical Chemistry

By

Iftikhar Ahmad

Department of Chemistry
Quaid-i-Azam University
Islamabad
2000

DECLARATION

This is to certify that this dissertation submitted by Iftikhar Ahmad in its present form is accepted by the Department of Chemistry, Quaid-i-Azam University, Islamabad as satisfying the dissertation requirements for the degree of **Master of Philosophy** in **Physical Chemistry.**

Supervisor

Dr. M. Sadiq Subhani
Associate Professor

External Examiner

Chairman
Department of Chemistry
Quaid-i-Azam Undiversity
Islamabad.

Prof. Dr. A. Y. Khan

DEDICATED

To

Hazrat

Muhammad

(Sallallaho Alaihe wa Alyhe Wasallum)

CONTENTS

ACKNOWLEDGEMENT

I owe my profound thanks and deepest sense of gratitude to Almighty ***Allah***, Creator of the universe, worthy of all praises, the merciful, Who blessed me with determination, potential and ability to complete this research work. I offer my humblest and sincere thanks to the Holy Prophet ***Muhammad*** (Sallallaho Alaihe wa Alyhe Wasallum) who exhorts his followers to seek knowledge from cradle to grave.

I am highly indebted to my affectionate supervisor ***Dr. M. Sadiq Subhani*** for supervising this work. His inspiring guidance, remarkable suggestions, constant encouragement, keen interest, constructive criticism and friendly discussion enabled me to complete the research and this thesis efficiently. I found him to be a very hardworking man, who settles for nothing less than perfection, which compelled me to work hard with his extremely challenging disposition to this arduous task.

I am greatly honored to pay my sincere thanks to ***Dr. Matiullah*** (P.S.O, PIEAS). I acknowledge with immense pleasure and want to express my feelings of indebtedness for his valuable guidance, inspiring criticism, zealous interest and personal involvement, which he displayed for this research work.

I am extremely grateful to the ***Pakistan Atomic Energy Commission***, for the provision of all possible facilities, full co-operation and excellent environment to accomplish this dissertation.

It is my pleasure to acknowledge the valuable assistance of ***Prof. Dr. A.Y. Khan***, Chairman, Department of Chemistry, Quaid-i-Azam University, Islamabad. It is his enthusiastic and encouraging effort that helped in doing my research work. The same is true for all other faculty members of the department especially all teachers of Physical Section, for their co-operation and moral support.

I wish to express my sincere thanks to ***Dr. Nasir Ahmad*** (C.S.O, PIEAS), ***Dr. S. M. Mirza*** (P.S.O, PIEAS) and especially ***Dr. Khalid Khan*** (S.S.O, PINSTECH) for useful discussions, moral support and guidance.

I don't find myself in a position to pay a tribute to ***Mr. M. Asif*** (S.A.I., PIEAS) and ***Mr. M. Javed Iqbal*** (S.A.I., PIEAS) for co-operation, guidance and assistance of whom has been countless and beyond the limits of my expression, which enabled me to complete this research work.

Special thanks are due to all my class fellows, ***Safeer Ahmed, Qaisar Mahmood Malik, Saira Irshad and Abbas Khan***, not only for extending their moral support but also for the memorable moments, which I shared with them during my stay at this University.

I extend my cordial thanks to my friends, ***Sheikh M. Iqbal Lasi***, ***Abid Mustafa*** and ***Irshad Ali*** . They are not only a continuous source of encouragement for me; they also shared with me too most jeering as well as most depressed moments of my life.

I am greatly indebted to ***Miss Bushra Naseem***, senior research fellow at Quaid-i-Azam University, Islamabad for extending co-operation in UV experimental work.

Last but not least, no words to describe my feelings of respect about my affectionate parents, brothers and sisters, for the understanding, unlimited support and encouragement they have shown through the past two years, I spent in doing this research. Without their prayers and affection, perhaps it could be impossible to attain this target.

(*Iftikhar Ahmad*)

ABSTRACT

In the field of solid state nuclear track detectors (SSNTDs), plastic CR-39 is the highly sensitive track recording material .The studies were carried out to see the effect of concentration of etchant (in the range of 4 to 12 M), different etchant and temperature (in the range 50-82 °C) on the bulk etch rate of CR-39.

The reported method for bulk etch rate determined (Henke Benton's method) was modified to remove the absorbed etchant and get better results with high accuracy and reduce the systematic error in bulk etch rate. It was also observed that the saturated etchant decreased the bulk etch rate. Whereas the water absorbed before exposure the detector enhances the bulk etch rate.

It was also found that the etchant concentration strongly effected on the alpha track diameters. Bulk etch rate of CR-39 depends upon the absorbed dose by γ-rays.

LIST OF TABLES

LIST OF FIGURES

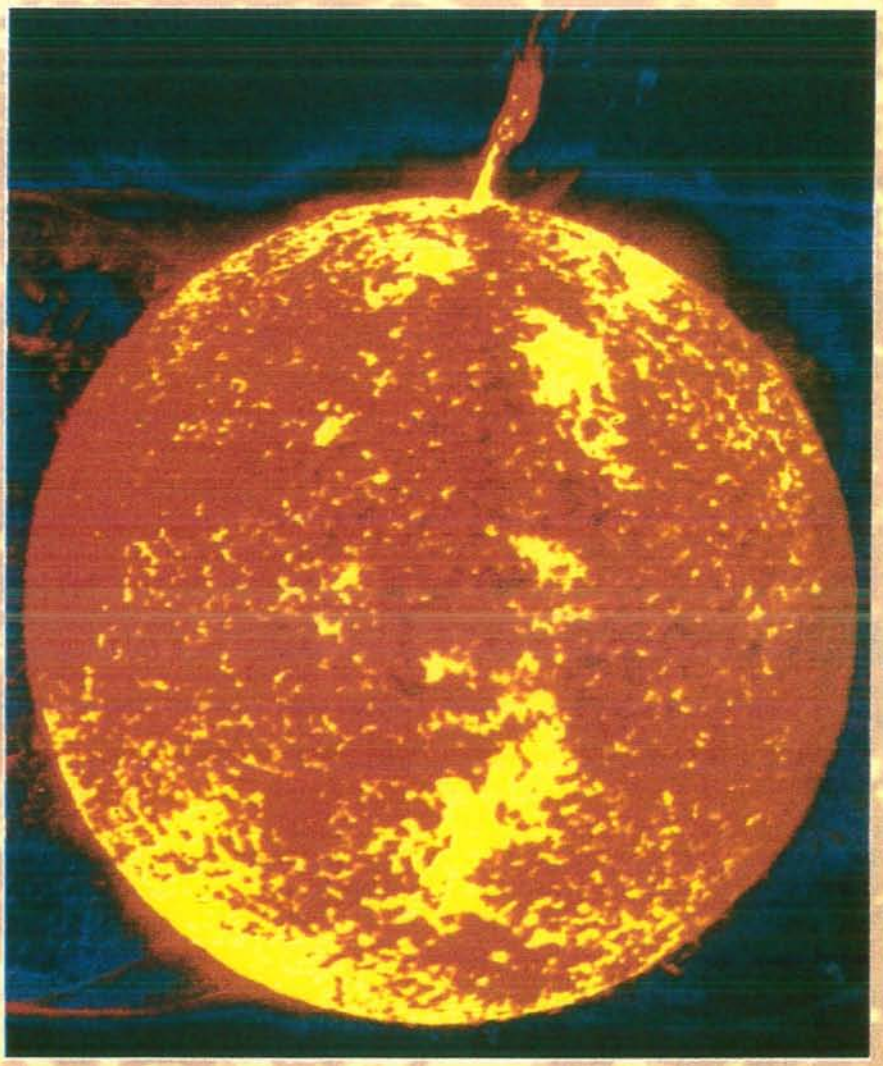

The sun is the source of life. Deep in its interior nuclear reactions are occurring that liberate life-giving energy.

Chapter # 1

INTRODUCTION

INTRODUCTION

One cloudy day of 1896, a French scientist Henri Becequerel[1] was unable to do an experiment, but he left the uranium on top of unexposed photographic film. Several days later, he developed the film anyway and discovered that the part underneath the uranium salt was exposed. Obviously, the uranium spontaneously emitted some form of radiation. It was this discovery that marked the true beginning of the nuclear age.

The discovery of natural radioactivity was a key that unlocked many of the mysteries of the atom. Since radiation causes destruction of living cells, it must be monitored in many locations or situations. Therefore scientists have developed many ways to detect, record, and measure radiations from radionuclides.

However, the durability, simplicity, low cost and markedly specific nature of the response of Solid State Nuclear Track Detectors (SSNTDs) led to their rapid application in a wide variety of fields[2].

1.1 SSNTD

When accelerated charge particles or heavy ionizing radiation pass through insulating media, trails of intense damage are produced, these trails are very narrow and can be studied by using an electron microscope. However, these damaged trails can also be visualized through an optical microscope by enlarging them chemically. The process of enlargement of the damaged trails is called chemical etching. These damage trails are called tracks and the materials retaining such tracks are called Solid State Nuclear Track Detectors (SSNTDs).

1.1.1 Early History of SSNTDs

SSNTDs enjoy a unique distinction of being the oldest and the youngest member of the nuclear particle detector family. They have been existing on the earth and the cold planets in the form of crystalline minerals and glassy matter for the last billion of years. However, they were discovered recently.

The process of track formation is older than the creation of man. However, the story of detection of charged particle tracks began in 1958, when D.A. Young working at the Atomic Energy Establishment in England, discovered that LiF crystals, held in contact with a uranium foil and irradiated with thermal neutrons, revealed a number of etch pits after treatment with a chemical reagent [3].

First time in 1959, Silk and Barnes, working in the same laboratory, observed hair like tracks using (in SSNTDs) electron microscope in thin sheets of mica. They have also observed that the fission fragment tracks which are less than 300 ^{o}A in diameter and greater than 4 um in length have been seen [4].

In 1961, P.B. Price and R.M. Walkers carried on work from the stage where Silk and Barnes had left. Afterwards in 1963, Fleischer joined the team of Price and Walker, and almost all the work on SSNTDs in earlier years was reported by them [5].

The application of track detectors to neutron dosimetry was first described by Walker et al.[6] in 1963. In 1965, Fleischer et al.[7] had

determined that, for tracks to form, the "electrostatic stress" must be greater than the "mechanical strength" of the material.

The earliest, and perhaps the most natural, explanation of track formation was that it depended on the total amount of energy deposited per unit path length by the incident ion. This criterion was proposed by Fleischer et al.[8].

In 1967, Price et al.[9] have first time, used the solid state nuclear track detectors for particle identification with the help of track etching rate V_T and the residual range R at which this etch-rate value was carried out.

In 1967, C.W. Naeser[10] has used the solid state nuclear track detectors as a tool for fission track dating.

In 1968, K Becker[11] has reported that during the irradiation of plastic, an increase of sensitivity was due to presence of oxygen. Oxygen is believed to combine with ions and radical and preventing their recombination.

To count the track density by optical microscope is a tedious work. To solve this problem Cross and Tommasino[12], have introduced the electronic spark counter technique first time in 1968. In 1968, P.B. Price et al.[13] have used the plastic track detectors for identification of cosmic rays. Track-rich grains in meteorites were first observed by Lal and Rajan (1969)[14].

The electrochemical etching method was developed by Tommasino[15] in 1970 .

In 1971 G. Crozaz et al.[16] have studied the lunar samples with the help of solid state nuclear track detectors.

Fleischer et al.[17] have determined a value for 2000 Ω cm as the limiting resistivity below which tracks are not observed. Frank and Benton[18] have used track-etch dosimeter to measure the radon levels in houses.

Small-angle X-ray scattering has been used to probe the nature of the crystal defects which comprise particle tracks[15].

Chambaudet et al.[19] have studied irradiated polymers, using electron spin resonance (ESR) spectroscopy, and have suggested that the existence of heavy-ion track might be correlated with the formation of carbon-like radicals similar to those produced in polymer pyrolysis.

Gore et al.[20] in 1978 have also introduced the SSNTDs in biological sciences. O'Sullivan[21] has been shown that track formation in polymers correlates with the G-value for molecular chain scission (i.e. the number of chain scission per 100 eV of energy deposited.

In 1978 Cartwright et al.[22] have introduced CR-39 in the field of SSNTDs, which have high sensitivity and good uniform response to the radiation.

1.1.2 CR-39 as a SSNTD

Most of the currently used SSNTDs, whether polymers, minerals, or glasses, suffer from being inhomogeneous and an isotropic with regard to their physical characteristics. These defects manifest themselves in non-geometrical surface hole openings, azimuthal dependence of response; differences between surfaces (of the same sheet) in sensitivity and bulk etch rate and surface pitting[23].

CR-39 is a plastic detector that has overcome many of the major problems associated with polymeric SSNTDs used to date. This plastic is thermoset, cross-linked, totally amorphous and very active to heavy-ion damage. It satisfies the requirements of (1), being typically transparent, (2) being very sensitive to radiation, (3) being highly isotropic and homogeneous, (4) not cross-linking after radiation damage has broken the chemical bonds and (5) having non-solvent chemical etchant (i.e. the etchant degrades the polymers instead of dissolving the material into solution)[24].

Thermoplastics are characterized by softening on heating, hardening on cooling being soluble in some solvents and having no strong bonds between individual macromolecules. In contrast, thermoset plastics, such as CR-39, are characterized by being hard, infusible and insoluble in all solvents[23].

1.1.3 Characteristics of CR-39

CR-39 is the trade name of allyl diglycol carbonate, whereas CR stands for "Columbia Resin"[25]. CR-39 has following most important properties

* **Absolute Clarity**

CR-39 has optical properties comparable to those of optical glass. Its surfaces are equal polished glass in luster and smoothness.

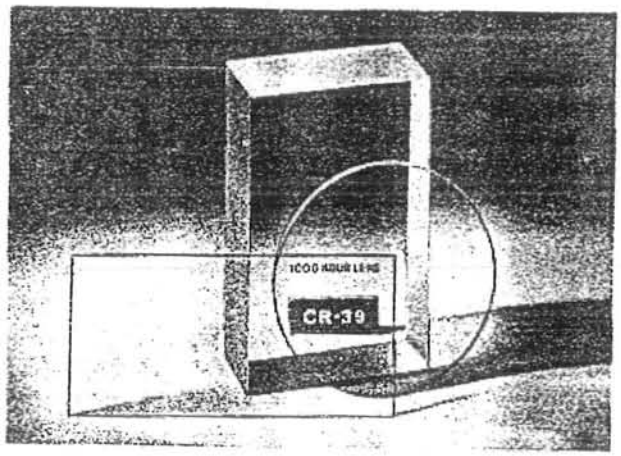

Fig. 1.1: Photographs of CR-39.

* **Exceptional impact resistance**

The impact strength of CR-39 at very low temperature is unusually good.

* **Chemical and solvent resistance**

CR-39 is immune to the effects of virtually all solvents and to most chemicals.

* **High heat resistance**

CR-39 resists distortion due to heat.

* **Light weight**

CR-39 has a specific gravity slightly lower than that of most plastics and approximately one-half that of glass.

1.1.4 Advantages of SSNTDs

SSNTDs have many advantages over the other detection techniques, which are describes in following[15].

(1) Simple in construction and use

(2) They are inexpensive

(3) The integrating nature of these detectors allow data (tracks) to be recorded over long periods of time.

(4) The recorded data can be revealed, at a convenient time, using simple chemicals for etching the tracks.

(5) In many applications they serve as threshold detectors because they are unaffected by high doses of background radiations of energy below the given threshold.

(6) As they do not involve any electronic accessories these are no problems with electrical noise or breakdown during long time data acquisition.

(7) Insensitive to light radiations

(8) High detection efficiency

1.1.5 Disadvantages of SSNTDs

All the observations require extensive use of microscope. This process is time consuming and human error is always present in the observation, which may effect the results. Automatic scanning systems are available commercially which can reduce the observations time but they are very costly[15].

Chapter # 2

TRACK FORMATION MECHANISM, CHEMICAL ETCHING AND TRACK GEOMETRY

TRACK FORMATION MECHANISM, CHEMICAL ETCHING AND GEOMETRY

Some general properties of CR-39 nuclear track detectors and history of SSNTDs were outlined in Chapter-1. Here a brief description of the track formation and development mechanisms in SSNTDs, as well as chemical etching and track geometry of nuclear track detectors will be discussed.

2.1 TRACK FORMATION MECHANISMS

When ionizing particles communicate energy to the stopping medium, the processes followed three stages. The first physical stage is followed by a physico-chemical stage, in which the initially generated primary products (i.e. ions; excited atoms and molecules; free electrons etc) rapidly undergo secondary reactions (dissociation of these excited molecules, etc), until the system reaches thermodynamic equilibrium. This is followed by the chemical stage, in which ions and free radicals react with each other to yield the final products of the irradiation[15].

2.1.1 Radiation Damage in Solids

The type of damage produced by irradiation of solids depends not only on the nature of ionizing radiation but also on the nature of the solid itself and the energy associated with radiations.

2.1.1.1 Polymers

Latent charged particle track production in polymers is essentially due to chemical bond breaking events along the ion trajectories. Ion-beam induced scission of polymeric chains typically produces charge redistribution along the skeletal backbone of a polymer molecule[26].

Charged particle tracks in many detectors arise from the interaction of delta rays with the sensitive elements of detector medium. This seems also to be the case for SSNTDs, and especially for polymers[27].

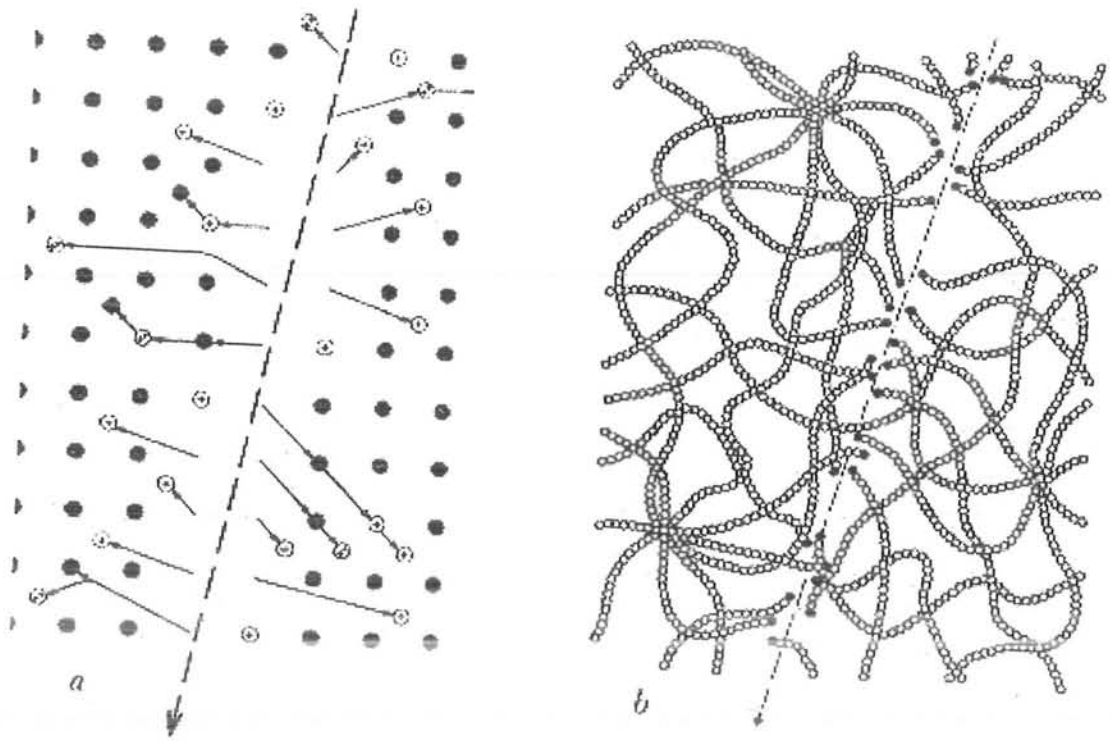

Fig. 2.1: (a) In crystal the damage consists of atomic displacement directly through elastic collisions. (b) The atomic character of particle tracks in the polymer, where the new ends and other chemically reactive sites are formed.

In the result of primary ionization the ejected electrons, if have sufficient energy to produce further excitation and ionization are called delta rays.

Katz and Kobetich[28] suggested that energy deposition by δ-rays is more important than the primary events themselves especially in polymers. The energy deposited by electrons at about 20 °A from the ion path is the

critical factor in determining whether or not a track is formed. The net effect on the plastic will be the production of many broken molecular chains, leading to a reduction in the average molecular weight of the substance.

2.1.1.2 Crystals and Glasses

The effect of radiation upon crystals and glasses will also be to produce ionization and excitation of atoms or molecules. The critical factor, which is responsible for track formation in crystals and glasses, is an atomic displacement through elastic collisions[29].

Thus the evidence suggests that the secondary effects of δ-rays are unimportant in inorganic solids. It was reported that the primary ionization appears to be the major source of track damage[30].

The overall conclusion to be drawn from the studies of track formation by ions of different energies is that tracks are generally formed by ions at energies for which electronic interactions are the dominant mode of energy loss. Etchable damage is usually not produced at the very end of the ion path where nuclear interactions become important[31].

2.2 CHEMICAL ETCHING

Latent tracks (damage) are not visible under an optical microscope. Direct viewing of damage trails was, in fact, achieved with a transmission electron microscope.

Certain chemical reagents ("etchants") dissolve or degrade these damaged regions at a much higher rate than the undamaged material. The narrow damage trail is thus gouged out by the etchant, forming a hole in cone shape that is called track[32].

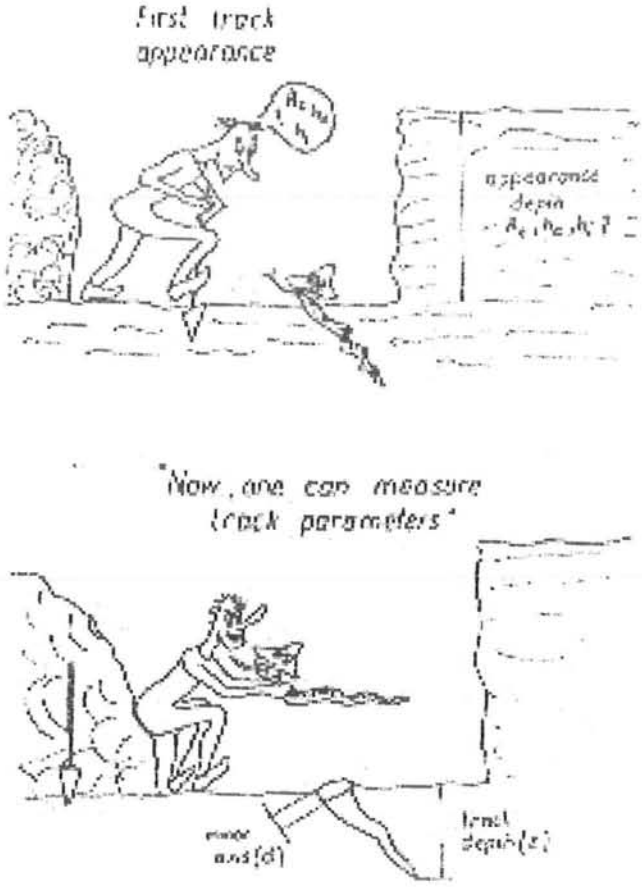

Fig. 2.2: Drawing illustrating an important behavior of track method.

Chemical etching is the most widely used method of "fixing" and "enlarging" the image of the latent damage trail in a solid state track detector. Essentially, etching takes place via rapid dissolution of the disordered region of the track core, which exists in a state of higher free energy than the undamaged bulk material[33].

The linear rate of chemical attack along the track is termed as "track etching rate", denoted by V_T. The surrounding undamaged material is attacked at a rate "V_B" which is called bulk etch rate. The bulk etching rate is generally constant for a given material and for a given etchant applied under a specific set of etching conditions[34].

2.2.1 Etching Conditions

For plastics, the most frequently used etchant is the aqueous solution of NaOH with concentrations in the range 1 to 12 M. The temperatures usually employed are in the range 40 - 70 °C. In some cases ethyl alcohol is added to the etchant for reducing the threshold value of primary ionization at which tracks become etchable[35]. In fact, this treatment also renders the plastic more brittle. However, alcohol has been found to reduce the sensitivity of CR-39.

In some studies KOH has been used. The mixed etchant solution of NaOH and KOH has also used in various ratios[36].

Glasses are almost invariable etched in aqueous HF solutions using 48 vol% HF at room temperature.

Etching time can vary from a few seconds (e.g. 48% HF on soda-lime glass) to many hours (for example, cosmic ray tracks in Lexan may require etching for 96 hours in 6.25 M NaOH at 40 °C)[37]. For obtaining work of high accuracy long etching time is preferable and control of temperature is often necessary[15].

If reproducible results are to be obtained, it is important that the quality of the etchant should be carefully controlled. After prolonged use high concentrations of etch products build up in the etchant. It is, therefore necessary to use fresh prepare etchant solution[34].

The process of chemical etching depends upon the following factors[38].

1. Type of solution (i.e. NaOH, KOH etc)
2. Concentration of etchant
3. Temperature of etchant
4. Etching time
5. Stirring rate during the etching
6. Number of interruption during etching
7. Reaction products
8. Environmental effects

2.2.2 Methods of Bulk Etch Rate Determination

The bulk etch "B" is the thickness of detector removed from each surface of SSNTD during its chemical etch processing. V_B is an especially important parameter for CR-39 detector because it serves to[39]

(i) Facilitate the reduction of the measured parameters of the tracks into quantities, which have more absolute significance.

(ii) Act as a calibration parameter for the detector and the etching process.

Three methods are mainly employed for the measurement of V_B depending upon the type of detector's material and facilities available.

(1) Thickness change method

This method is based on the direct measurement of change in thickness of the detector due to etching process[40].

$$V_B = \frac{t_2 - t_1}{2t} \quad (2.1)$$

Where

t_1 = thickness of the detector before etching

t_2 = thickness of the detector after etching

t = etching time

(2) Fission fragment tracks diameter method

In this method, the diameters of the fission fragment tracks are measured under optical microscope and bulk etch rate is found as[41].

$$V_B = \frac{D_f}{2t} \quad (2.2)$$

Where "D_f" is the fission fragment track diameter.

(3) Mass change method (Henke Benton's method)

This method is based on the measurement of the mass change of the detector during etching.

The total bulk etch "B" is obtained from the following relationship[39]

$$B = \frac{(m_1 - m_2)t_2}{2m_2} \frac{[1 - Pt_2]}{2A} \quad (2.3)$$

Where

m_1 = the mass of detector before etching

m_2 = the mass of detector after etching

t_1 = the thickness of detector before etching

t_2 = the thickness of detector after etching

t = etching time

A = area of the detector

P = Perimeter of the detector

B = bulk etch

It was reported that among above mentioned three methods of V_B measurement, the use of the mass change method provide a very consistent and reliable measurement of V_B[39].

2.2.3 Activation Energy

The etching process is a diffusion process and the bulk etch rate (V_B) essentially depends on temperature. An exponential dependence of V_B on temperature T is given by the relation[42].

$$V_B = A\, e^{-E_b / kT} \qquad (2.4)$$

Where A is constant, E_b the activation energy for bulk etching process and k, the Boltzman constant. Activation energy of bulk etch is defined as the minimum energy required to activate the reaction between the detector material and the etchant solution.

2.2.4 Chemistry of Track Etching

The chemical composition of the reaction products of CR-39 (allyl diglycol carbonate) and aqueous NaOH has been studied and reported in the literature[43]. It has been found that attack by the hydroxide ion results in the hydrolysis of the carbonate bonds and the release of poly-allylalcohol (PAA) from the polymer network. The reaction is

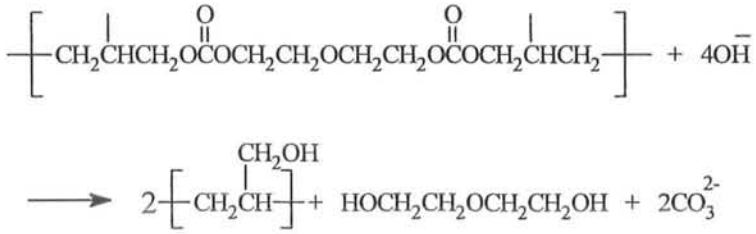

(2.5)

In addition to the polymeric etch product PAA, 2,2′-oxydiethanol is also formed in the reaction (2.5).

The gel permeation chromatography (GPC) analysis of the etch products was used to identify the radiation sensitive link in the CR-39 network. This helped to conclude that it is diethyleneglycol dicarbonate link in the CR-39 network which is in fact radiation sensitive and is responsible for the increase of the etch rate in the radiation damage plastic[44].

2.3 TRACK ETCHING GEOMETRY

The application of SSNTDs in science and technology requires sufficient knowledge of track geometry.

The geometry of track etching is described in the simplest case by the simultaneous action of two etching processes: chemical dissolution along the particle track at a higher rate V_T and general attack on the etched surface at a lower rate V_B[45].

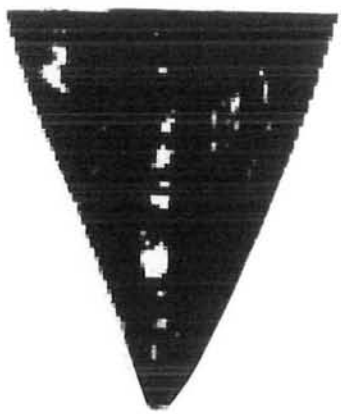

Fig. 2.4 Illustrates how this process create a cone having the original track as its axis.

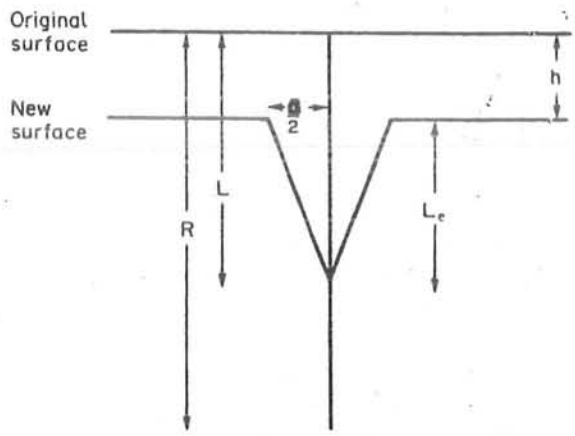

Fig. 2.5: Some parameters use to describe the geometry of etched tracks. R, full length of the unetched track; L, the length of track attacked by the etchant up to a given movement; L_e, the observed length of the etched track; h, the thickness of the surface removed by etching; D, the track diameter.

The most easily measurable parameters of an etched track are the bulk etch rate "V_B" and track diameter "D". The track etch rate V_T, is determined by using the relationship[46].

$$V_T = V_B \frac{4h + D^2}{4h - D^2} \qquad (2.6)$$

h = thickness of the detector removal after etching (i.e. $h = V_b t$)

D = track diameter

The track etching parameters (e.g. the sensitivity, the etching efficiency and critical angle of etching) have been determined using the following relationships (2.7 to 2.9)[15].

$$\text{Sensitivity, } S = \frac{V_T}{V_B} \tag{2.7}$$

$$\text{Track etching efficiency, } \eta = 1 - (V_B / V_T) \tag{2.8}$$

$$\text{Critical angle of etching } \theta_c = \text{Sin}^{-1} (V_B / V_T) \tag{2.9}$$

In the field of SSNTDs, the sensitivity, (S) given by the ratio of the rate of etching along the path of the damaged trail to the rate of etching of the undamaged material, is the most important parameter. Higher the sensitivity better is the detector[15].

The track etching efficiency is one of the most important criteria in the choice of a detector. As the etching efficiency (η) depends upon the ratio V_B / V_T it is clear that higher the efficiency (η), better is the detection limitation of the detector[47].

The angle θ_c is known as the critical angle of V_T etching and represents the minimum angle to the surface that a track can make in order to be revealed by etching[48].

Range of the particles reported in the literature can also be described as (2.10)[49].

$$R = V_T \, t_o \tag{2.10}$$

Where

R is the range length of the particle from the original top of the sample and t_o is the time of etching when the etchant reaches the end of the latent damage trail.

The purpose of the study of etched track geometry is to relate these parameters such as the bulk etch rate (V_B), track etch rate (V_T) and particle range in detector (R) to the quantities of interest such as Z, M or β may ultimately be deduced[15].

Chapter # 3

SSNTD APPLICATIONS IN SCIENCE AND TECHNOLOGY

SSNTD APPLICATIONS IN SCIENCE AND TECHNOLOGY

The emergence of Solid State Nuclear Track Detectors (SSNTDs) as a new means of charged particle detection in the late fifties [3] was followed by a phase of rapid expansion in the applications of this technique. The pioneers of this field, specially the famous trio of Fleischer, Price and Walker[50], worked with zeal and imagination to introduce new uses of track detectors in different areas of science and technology.

In recent years SSNTD have been established as a scientific tool with wide variety of applications in different areas of science and technology[15].

In this chapter, in spite of the remarkable diversity of SSNTD applications, some of these applications with the special reference of science and technology have been discussed.

3.1 NUCLEAR SCIENCE

3.1.1 Heavy ion nuclear reactions

Gottschalk et al.[51] have initiated the quantitative analyses of heavy ion reactions. Gottschalk et al. [52] have been recently reported a large number of heavy ion nuclear reactions along with data on

⇒ Total and partial cross-sections

⇒ Elastic scattering angular distributions and derivation of quarter point angles,

⇒ Determination of reaction mechanism such as deep inelastic scattering and sequential fission, and

⇒ Masses, kinetic energies, and angular distributions of the reaction products in intermediate and final reaction steps.

3.1.2 Fission studies

SSNTD applications in basic research relevant to Nuclear Physics and Nuclear Chemistry have been dominated by fission studies. Beginning with the earliest ground breaking observations of fission tracks in mica, the track detectors were used to generate the data of historical importance on spontaneous fission half-lives, life-times of compound nuclei, fission cross sections and fission barrier heights. [53]

3.1.3 Complex radioactivity

Complex radioactivity or cluster radioactivity occurs along with α–decay [54].

The majority of cluster decay modes observed were reported on the basis of data obtained with higher accuracy by SSNTD technique. A detailed overview of cluster radioactivity results based on SSNTDs is available in the literature[55].

3.2 GEOLOGY/ GEOPHYSICS

3.2.1 Fission track dating

The fission tracks in crystals represent the age when the crystal was cooled below the closure temperature. Different crystals within a given rock would yield widely different ages of the rock if there were significant difference of closure temperature. This fact can also be used advantageously to estimate the uplift history of mountain ranges[53].

An example of a good age determination is the work reported by Guo et al. (1997)[56].

This work is also relevant to Archaeology since tektites were found near the habitat Chinese ancient man. The technique of fission track dating is widely used for the study of archaeological remains of old civilizations[57] The track dating method applied on lunar samples and meteorites[14,16].

3.2.2 Petroleum and oil prediction

R.L. Fleischer (1998) [58] has identified the thermal history of rocks studies with SSNTDs as one of the most potentially profitable commercial use of track detectors because of its relevance to petroleum geology. The tracks of spontaneous fission fragments in minerals are shortened and the track etching rate is reduced due to high temperature episode experienced by a given rock formation. Such rocks are not likely to bear oil deposits. Therefore an expensive deep drilling process can be avoided in regions with unfavorable thermal history [59].

3.2.3 Geophysical applications

Apart from fission track dating and thermal history of rocks, a number of other geological studies are prone to track detection technique, e.g. searching for geothermal energy sources, location of main boundary faults and prediction of earthquakes [60]

3.3 ENVIRONMENTAL SCIENCE

3.3.1 Radon dosimetry

Measurements of radon levels to monitor and control indoors radioactive pollution continue to be activity pursued by the users of SSNTDs. The current status of developmental work on radon dosimetry involves SSNTD technology[61].

3.3.2 Neutron dosimetry

This is an area where track detection has its most useful applications in nuclear technology as well as in other nuclear establishments[62].

The neutrons themselves do not leave tracks in dielectric solids, however, their secondary effects, thermal neutrons are detected by the neutron-induced fission in ^{235} U. Here fission fragments are registered in the track detector. Neutrons may also induce (n, α) reactions in certain materials. Such as ^{6}Li (n, α) ^{3} H and ^{10}B (n, α) ^{7} Li. (N. Ahmad et al 1997) [63]. The resulting α– particles are registered in the detector giving a track count in directly proportion to the neutron flux.

The response of the detector has been shown to be smooth enough, in the form of track density for dose measurements, and that of track lengths for the identification of neutron energy.

3.4 MATERIAL SCIENCE

During the last two decades, research in the field of solid state nuclear track detectors (SSNTDs) has provided material scientists and technologists with new techniques for the characterization and micromachining of the materials.

The application of ion tracks in polymers, glasses and crystals in technology includes[64].

⇒ Change of bulk material properties (texture, optical properties, production of nuclear filter, etc.)

⇒ Influence of local properties (single – pore membranes and pinhole apparatus production, etc.)

⇒ Production of new devices in micro technology (electron devices, micro – Composite materials, etc.).

3.5 NUCLEAR TRACK FILTERS

Nuclear Track Filters (NTF) with well-defined pores have been studied for several years. Such filters are produced by heavy ions from accelerators and nuclear reactors and subsequent etching with appropriate chemical solution. The ideal pores structure, uniform pore size and nearly cylindrical pore geometries – makes them unique tools in modern science and technology [65].

3.6 PARTICLE RADIOGRAPHY

Because of its high sensitivity and good etching behavior, the CR-39 track detector should be useful in neutron, proton and heavy particle radiography. The high optical contrast between tracks and background should be very useful in delineating the radiographed image[66].

3.7 PARTICLE IDENTIFICATION

Solid State Nuclear Track Detectors have become quite popular in recent years as an alternative tool for the identification of charged particles produced in nuclear reactions, principally because of the availability of highly sensitive plastics like CR-39 thus can register tracks produced by protons to transuranium elements in the range of very low to very high energies[67].

3.8 ASTROPHYSICS

3.8.1 Cosmic rays

An area of intense SSNTD usage has been the study of elemental and isotopic composition of primary galactic cosmic rays. A long series of experiments on cosmos series, Russian satellites and NASA have been monitoring cosmic ray heavy nuclei with energies from 100 to 800 MeV/ nucleon, since 1973. A compact summary of their results has been reported in literature [68].

3.8.2 Lunar sample studies

One of the most exciting application of the track-etch method during the last decade has been the investigation of lunar-surface processes and of ancient solar and galactic radiation through the examination of fossil tracks in lunar rocks and soils provided by the Apollo and Luna missions flown by the USA and the USSR, respectively[69].

3.8.3 Meteorites

Track-rich grains in meteorites were first observed by Pellas et al[14] Meteorites rich in rare gases usually also contain track- rich grains. Both of these features are believed to be the result of irradiation, by the solar win and solar flares, of an ancient meteoritic soil layer.

3.9 BIOLOGICAL APPLICATIONS

3.9.1 Inhalation of α-active particles

Much interest has been taken, in recent years, in the radiological consequences of the inhalation of α-active particles (present in tobacco smoke or in the atmosphere of uranium mines) and their deposition in the lung. The sections of bronchus between sheets of CR-39 were sandwiched

for 3-4 months and then etched the plastic to reveal α-particle tracks produced by radioactive particles lodged in tissue[70].

These studies were further extended to the monitoring of α-activity in the bloodstream by immersion of CR-39 detectors in fresh blood taken from smoking and non-smoking persons [71].

3.9.2 Lead in teeth

Fremlin and co-workers have used SSNTD techniques to measure the spatial distribution of lead in human teeth, and in particular to study the lead content as a function of the person's age [72].

3.10 AIM OF WORK

As described earlier after the discovery of CR-39, it dominated the field of SSNTDs due to its high detection sensitivity and uniform response.

It is reported in literature CR-39 swells during etching due to absorption of etchant, it causes serious systematic error in V_B measurement by mass change method.

The purpose of work presented here is to develop an modified method for V_B measurement with ability to minimize the above mentioned problem.

To study the quantitative effect of saturated etchant as well as the effect of absorbed water by CR-39 before exposure on V_B also include in the aim of presented work.

Chapter # 4

EXPERIMENTAL

EXPERIMENTAL

4.1 EQUIPMENTS USED

As mentioned earlier (see Chapter-1), the simple instrumentation are needed for SSNTD, a brief introduction of them is being given below.

4.1.1 Optical microscope

For the measurements of track diameters and track densities, the carl zeiss optical microscope has been used.

The measurement of fission or alpha track diameters under the zeiss microscope is relatively simple, for this purpose the following accessories are used.

(i) Eyepiece micrometer

(ii) Net micrometer

(iii) Stage micrometer

The stage micrometer is a scale graduated in units of 10 μm on a conventional specimen slide.

Eyepiece micrometer has been calibrated with the help of stage micrometer at 10^3 times magnification, i.e. one small interval at eyepiece micrometer equal to 1 μm.

Whereas for track density measurement the net micrometer has been used.

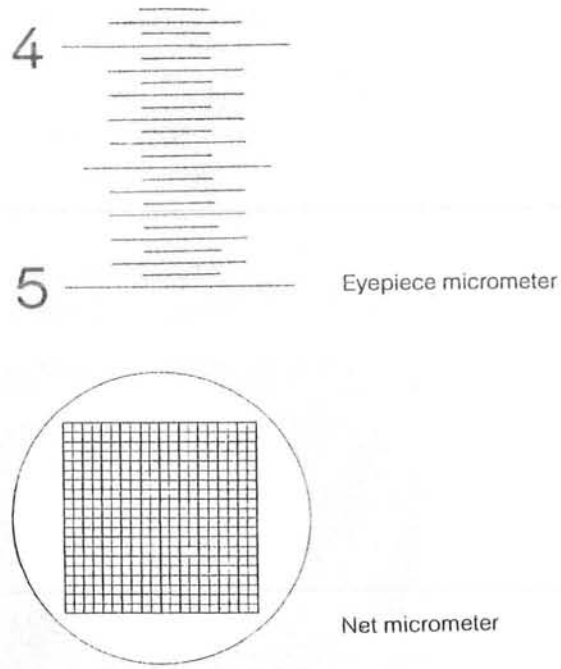

Fig. 4.1: Eyepiece and net micrometer.

4.1.2 Furnace

The detectors were completely dried by using the carbolite furnace. The carbolite furnace has the ability to heat up to 1200 °C.

4.1.3 Etching bath

The Gallenkamp etching bath was used. The detectors have etched in Gallenkamp etching bath. The temperature of etching bath was controlled from 20 to 100 °C, whereas the shaking speed was controlled in the range 20 to 200 RPM.

4.1.4 Analytical balance

The Metter Analytical balance AE200 was used for weighing the detectors with accuracy of 0.1 mg.

4.1.5 Spectrophotometer

To obtain the UV spectra, the Perkin Elmer UV/Vis spectrometer (Lambda 20) was used.

4.2 Radiation sources used:

To exposed the CR-39 detectors the following radiation sources were used as shown in Table 4.1

Table 4.1: Radiation Sources Used.

S.No.	Source	Decay Mode	Half-life	Energy
1.	^{241}Am	α-particles	433 y	5.485 MeV
2.	^{252}Cf	α-particles spontaneous fission	2.73 y 85.5 y effective half life - 2.65 y	6.217 MeV 185 MeV
3.	^{60}Co	γ-rays	5.26 y	1.73 MeV 1.332 MeV

4.3 CHEMICALS USED:

The chemicals used, their purity grades and the manufacturers are given under:

Chemicals	Purity grade	Manufacturers
1. Water	Doubly distilled from $KMnO_4$ solution.	-
2. NaOH	97.0%	Fluka AG, Buchs SG, Switzerland.
3. KOH	98.0%	"
4. $C_2H_2O_4.2H_2O$	99.0%	"

All chemicals were used as such without further purification. The solutions were prepared in distilled water. The solutions of NaOH and KOH were standardized against oxalic acid, where phenolphthalein was used as an indicator.

4.4 EXPERIMENTAL PROCEDURES

To study the efficiency of CR-39 based dosimeters; the experiments were carried out in series of steps. Various aspects of CR-39 based dosimeters were studied. Experimental work for each aspect has been described separately.

4.4.1 An improved method for bulk etch rate "V_B" determination.

Large sheets of CR-39 detectors (12.7 cm x 12.7 cm), supplied by Pershore Mouldings Ltd., UK., were cut into small pieces of sizes 3.0 cm x 2.5 cm.

Two sets of CR-39 detectors (3.0 cm x 2.5 cm) were weighed using analytical balance. The thickness was measured by micrometer with precision of 1 um.

Now the CR-39 detectors were exposed to α-particles from the radioactive source ^{241}Am (5.4 MeV) for period of two minutes.

Irradiated detectors were etched in 6M NaOH at constant temperature of 70 °C with 60 Rev/m in shaking. In order to achieve the accuracy of method, the irradiation and etching conditions were kept the same. After two hours the etched detectors were washed in running water then with distilled water.

Now one set of CR-39 detectors were dried in folds of tissue papers, whereas the second set of CR-39 detectors were put into furnace at 80 °C (±1 °C) for complete dryness (80 to 90 min).

Both the sets of CR-39 detectors were weighted and measured their thickness.

Finally the bulk etch rate "V_B" of both the sets were determined by mass change method.

Above-mentioned process from etching to the determination of bulk etch rate was repeated (for both the sets of CR-39 detectors) further three times even the complete etching took 8 hours.

4.4.2 The effect of saturated etchant on bulk etch rate "V_B"

Two sets of CR-39 detectors (3.0 cm x 2.5 cm) were exposed to α-particles using ^{241}Am (5.4 MeV) for two minutes.

One set of CR-39 detectors were etched in freshly prepared 6M NaOH (unsaturated etchant) at 70 °C with 60 Rev/m in.

The second set of CR-39 detectors were etched in 6M NaOH in already saturated with etched products (saturated etchant) at 70 °C with 60 Rev/m in.

Both the sets of CR-39 detectors were washed using running water then with distilled water.

Now both the sets were put into furnace at 80 °C (±1 °C) for 80 to 90 min.

Before and after etching the mass and thickness of the detectors were measured with same procedure as mentioned already (in 4.4.1).

The bulk etch rate "V_B" was measured by mass change method.

4.4.3 The effect of concentration on bulk etch rate

Five sets of CR-39 detectors (3.0 cm x 2.5 cm) were exposed to α-particles using ^{241}Am (5.4 MeV) for two minutes each detector.

Now CR-39 detectors were etched in 4M, 6M, 8M, 10M and 12M NaOH respectively at 70 °C with 60 Rev/m in.

After etching all detectors were washed in running water then with distilled water.

Now all five sets put into furnace for complete dryness at 80 °C (±1 °C) for 80 to 90 min.

Before and after etching the mass and thickness of the detectors were measured.

The bulk etch rate "V_B" was measured by mass change method.

The track diameters of α-particles were measured for each set of CR-39 detector under the zeiss optical microscope using calibrated eyepiece micrometer.

The track etch rate "V_B" was determined by expression 2.3.

4.4.4 Activation energy of bulk etch process:

Eight sets of CR-39 detectors were exposed to α-particles using ^{241}Am (5.4 MeV), each detector for two minutes.

Four sets of CR-39 detectors were etched in NaOH. One set of CR-39 from above four sets were etched in 6M NaOH at 50 °C, 2nd set in 6M NaOH at 60 °C, 3rd set in 6M NaOH at 70 °C and 4th set in 6M NaOH at 80 °C with 60 Rev/min for each set.

Other four sets of CR-39 detectors were etched in KOH. One set of CR-39 detectors were etched in 6M KOH at 50 °C, 2nd set in 6M KOH at 60 °C, 3drd set in 6M KOH at 70 °C and 4th set in 6M KOH at 80 °C with 60 Rev/min for each set.

After etching all the sets were first washed in running water and then by distilled water.

The detectors were placed in the furnace at 80 °C (±1 °C) for 80 to 90 min.

Before and after etching the mass and thickness of the detectors were measured in each case.

The bulk etch rate V_B were measured by mass change method.

The track diameters of α-particles were measured for each set of CR-39 detector under the zeiss optical microscope using calibrate eyepiece micrometer.

The track etch rate "V_T" were determined using equation 2.3.

The activation energy of bulk etch rate was determined by using equation 2.1.

4.4.5 Determination of bulk etch rate by fission diameter method:

Two sets of CR-39 detectors (3.0 cm x 2.5 cm) were exposed to fission fragments of ^{252}Cf for 17 hours.

One set of CR-39 was etched in 6M NaOH at 70 °C with 60 Rev/min. 2nd set of CR-39 were etched in 6M KOH at 70 °C with 60 Rev/min.

After etching the detectors were washed in running water then distilled water and dry with tissue papers.

Fission and α-particle tracks diameter were measured by zeiss optical microscope.

The bulk etch rate "V_B" was measured by fission track diameter method.

4.4.6 The effect of water on bulk etch rate:

Two sets of CR-39 detectors were put into distilled water for 24 hours. After 24 hours detectors were dried with tissue paper and exposed to fission fragments of ^{252}Cf for 17 hours.

One set of CR-39 were etched in 6M NaOH at 70 °C with 60 Rev/min shaking. 2nd set of CR-39 were etched in 6M KOH at 70 °C with 60 Rev/min shaking.

After etching they were washed and dried as described already. Fission and α-particle tracks diameters were measured by zeiss optical microscope.

The bulk etch rate "V_B" was measured by fission track diameter method.

4.4.7 γ-Rays dosimetry

Sixteen CR-39 detectors (3.0 cm x 2.5 cm) were exposed with γ-rays. All detectors were absorbed different high gamma doses ranging from 1 Krad to 500 krad using a ^{60}Co gamma source. The dose rate was approximate 4.28 Krad h^{-1}. (The detectors mentioned above were irradiated using facilities at PARAS, Lahore.

All the detectors were etched in 6M NaOH at 70 °C with 60 Rev/min (The freshly prepared solution of 6M NaOH was applied for each pair of detector.

After etching the detectors were washed in running water then distilled water.

The mass and thickness were measured before and after etching. The bulk etch rate "V_B" was measured by mass change method.

Chapter # 5

RESULTS AND DISCUSSION

RESULTS AND DISCUSSION

The results obtained from experimental work are described in the form of following tables and figures.

Table 5.1: Data obtained using complete drying method, CR-39 was exposed from ^{241}Am and etched in 6M NaOH at 70°C.

m_1 (gm)	t_1 (μm)	Etching time (h)	m_2 (gm)*	t_2(μm)**	A (μm^2)	P (μm)	B (μm)
0.4861	493	2	0.4800	492	7655178	110998	3.0147
"	"	4	0.4750	489.33	"	"	5.514
"	"	6	0.4702	483.66	"	"	7.89
"	"	8	0.4657	481	"	"	10.167

Symbols used in tables are denoted as;

m_1 = the mass of detector before etching
m_2 = the mass of detector after etching
t_1 = the thickness of detector before etching
t_2 = the thickness of detector after etching
t = etching time
A = area of the detector
P = Perimeter of the detector
B = bulk etch

---

* Mass of the detector after etching where the detector was complete dried in furnace.
** Thickness of the detector after etching where the detector was complete dried in furnace.

Table 5.2: Experimental data for the measurement of V_B by Henke Benton's method, CR-39 was exposed from ^{241}Am and etched in 6M NaOH at 70 °C

m_1 (gm)	t_1 (μm)	Etching time (h)	m_2 (gm)*	t_2(μm)**	A (μm^2)	P (μm)	B (μm)
0.5004	501.33	2	0.5010	504	769980000	111332	-
"	"	4	0.4964	499.66	"	"	1.940
"	"	6	0.4919	494.66	"	"	4.120
"	"	8.25	0.4863	492.33	"	"	6.880

* Mass of the detector after etching where the detector was dried using tissue papers.

** Thickness of the detector after etching where the detector was dried using tissue papers.

Table 5.3: Experimental data for the effect of saturated etchant on V_B, CR-39 was exposed from ^{241}Am, etched in saturated 6M NaOH at 70 °C.

m_1 (gm)	t_1 (μm)	Etching time (h)	m_2 (gm)	t_2(μm)	A (μm^2)	P (μm)	B (μm)
0.4832	483.66	2	0.4774	484.33	774333000	111732	2.83
"	"	4	0.4730	480.33	"	"	4.99
"	"	6	0.4682	476	"	"	7.36
"	"	8	0.4639	472.33	"	"	9.49

Table 5.4: CR-39 was exposed from ^{241}Am, etched in 4M NaOH at 70 °C.

m_1 (gm)	t_1 (μm)	Etching time (h)	m_2 (gm)	t_2(μm)	A (μm^2)	P (μm)	B (μm)
0.4795	487.66	2	0.4755	486.33	765533300	111066	1.97
"	"	4	0.4729	484.66	"	"	4.26
"	"	6	0.4705	481.33	"	"	4.44
"	"	8	0.4681	480.33	"	"	5.64

Table 5.5: CR-39 was exposed from ^{241}Am, etched in 8M NaOH at 70 °C

m_1 (gm)	t_1 (μm)	Etching time (h)	m_2 (gm)	t_2(μm)	A (μm^2)	P (μm)	B (μm)
0.4994	501.5	2	0.4886	497.33	769261878	111398	5.29
"	"	4	0.4805	492	"	"	9.33
"	"	6	0.4719	484	"	"	13.6
"	"	8	0.4632	475.66	"	"	17.48

Table 5.6: CR-39 was exposed to α-particles from ^{241}Am, etched in 10M NaOH at 70°C.

m_1 (gm)	t_1 (μm)	Etching time (h)	m_2 (gm)	t_2(μm)	A (μm^2)	P (μm)	B (μm)
0.4805	492.6	2	0.4683	486.33	757304900	110466	6.1
"	"	4	0.4540	471.66	"	"	13.29
"	"	6	0.4393	458	"	"	20.76
"	"	8	0.4257	446.66	"	"	27.81

Table 5.7: CR-39 was exposed to α-particles from ^{241}Am, etched in 12M NaOH at 70°C.

m_1 (gm)	t_1 (μm)	Etching time (h)	m_2 (gm)	t_2(μm)	A (μm^2)	P (μm)	B (μm)
0.4940	505	2	0.4746	491	759499800	110732	9.67
"	"	4	0.4528	492	"	"	21.57
"	"	6	0.4299	449.66	"	"	32.42
"	"	8	0.4299	426.66	"	"	42.83

Table 5.8: The effect of concentration on bulk etch rate "V_B" CR-39 etching was at 70 °C*.

S.No.	Concentration of etchant C (M)	log C	Bulk etch rate V_B (um/h)	log V_B
1	4	0.602	0.609	-0.215
2	6	0.778	1.192	0.076
3	8	0.903	2.042	0.310
4	10	1.00	3.63	0.559
5	12	1.079	5.516	0.741

* Bulk each ratio was obtained from Fig. 5.9.

Table 5.9: CR-39 exposed to α-particles from ^{241}Am, etched in 6M NaOH at 50 °C.

m_1 (gm)	t_1 (μm)	Etching time (h)	m_2 (gm)	t_2(μm)	A (μm^2)	P (μm)	B (μm)
0.4848	486.3	2	0.4824	488	768915889	111332	1.171
"	"	4	0.4812	488	"	"	1.759
"	"	6	0.4801	486	"	"	2.295
"	"	8	0.4790	486	"	"	2.838

Table 5.10: CR-39 exposed to α-particles from ^{241}Am, etched in 6M NaOH at 60 °C.

m_1 (gm)	t_1 (μm)	Etching time (h)	m_2 (gm)	t_2(μm)	A (μm^2)	P (μm)	B (μm)
0.4855	496	2	0.4812	495	761136400	110732	2.133
"	"	4	0.4790	494	"	"	3.231
"	"	6	0.4765	491.33	"	"	4.474
"	"	8	0.4738	489	"	"	5.823

Table 5.11: CR-39 exposed to α-particles from ^{241}Am, etched in 6M NaOH at 82 °C.

m_1 (gm)	t_1 (μm)	Etching time (h)	m_2 (gm)	t_2(μm)	A (μm^2)	P (μm)	B (μm)
0.4912	486	2.066	0.4787	481.33	781983000	112332	6.067
"	"	4.033	0.4701	473	"	"	10.254
"	"	6.033	0.4600	464.33	"	"	15.221
"	"	8	0.4517	456	"	"	19.298

Table 5.12: The effect of temperature on bulk etch rate "V_B" etching was proceed at constant concentration (i.e. 6M NaOH).

S.No.	Temperature T(°C)	Bulk etch rate V_B (μm/h)
1	50	0.276
2	60	0.6156
3	70	1.192
4	82	2.255

Table 5.13: CR-39 exposed to α-particles from ^{241}Am, etched in 6M KOH at 50°C.

m_1 (gm)	t_1 (μm)	Etching time (h)	m_2 (gm)	t_2(μm)	A (μm^2)	P (μm)	B (μm)
0.4819	488.33	2	0.4792	487	766890278	111198	1.323
"	"	4	0.4777	487	"	"	2.063
"	"	6	0.4763	486	"	"	2.756
"	"	8	0.4749	486	"	"	4.455

Table 5.14: CR-39 exposed to α-particles from ^{241}Am, etched in 6M KOH at 60°C.

m_1 (gm)	t_1 (μm)	Etching time (h)	m_2 (gm)	t_2(μm)	A (μm^2)	P (μm)	B (μm)
0.4835	484	2	0.4784	483	771296400	111532	2.484
"	"	4	0.4757	480	"	"	3.798
"	"	6	0.4722	477.33	"	"	5.514
"	"	8	0.4693	475	"	"	6.939

Table 5.15: CR-39 was exposed to α-particles from ^{241}Am, etched in 6M KOH at 70°C.

m_1 (gm)	t_1 (μm)	Etching time (h)	m_2 (gm)	t_2(μm)	A (μm^2)	P (μm)	B (μm)
0.4846	490	2	0.4762	488	761674156	110864	4.151
"	"	4	0.4706	483	"	"	6.931
"	"	6	0.4647	476.66	"	"	9.852
"	"	8	0.4589	471	"	"	12.736

Table 5.16: CR-39 was exposed to α-particles from ^{241}Am, etched in 6M KOH at 82 °C.

m_1 (gm)	t_1 (μm)	Etching time (h)	m_2 (gm)	t_2(μm)	A (μm^2)	P (μm)	B (μm)
0.4971	504	2.066	0.4811	495.33	765729800	111132	7.94
"	"	4.033	0.4694	484.33	"	"	13.788
"	"	6.033	0.4560	472.33	"	"	20.556
"	"	8	0.4443	461	"	"	26.475

Table 5.17: The effect of temperature on bulk etch rate "V_B", etching was proceed at constant concentration (i.e. 6M KOH).

S.No.	Temperature T (°C)	Bulk etch rate V_B (μm/h)
1	50	0.354
2	60	0.754
3	70	1.433
4	82	3.149

Table 5.18: Activation energy (E_B) for bulk etching, whereas CR-39 was exposed from ^{241}Am and etched in 6 M NaOH.

V_B (μm/h)	$\ln V_B$	T (°C)	1/T (K^{-1}) x 10^{-3}	Slope* = $-E_B/k$	E_B (eV)
0.276	-1.284	50	3.09	-7460.08	0.64
0.615	-0.485	60	3.00		
1.192	0.1747	70	2.91		
2.255	0.813	82	2.81		

* Slope was obtained from the plot of $\ln V_B$ Vs 1/T (see Fig. 5.14).

Table 5.19: Activation energy (E_B) for bulk etching, whereas CR-39 was etched in 6M KOH

V_B (μm/h)	$\ln V_B$	T (°C)	1/T (K^{-1}) x 10^{-3}	Slope* = $-E_B/K$	E_B (eV)
0.354	-1.037	50	3.09	-7735	0.66
0.754	-0.282	60	3.00		
1.433	0.360	70	2.91		
3.149	1.147	82	2.81		

* Slope was obtained from the plot of $\ln V_B$ Vs 1/T (see Fig. 5.15).

Table 5.20: Determination of bulk etch rate by fission track diameter method CR-39 was exposed from ^{252}Cf, etched in 6M NaOH 70 °C. ($V_B = D_f / 2t$)[41].

Etching time t(h)	Fission fragments tracks diameter D_f(μm)	α-particle tracks diameter D_α (μm)	V_B = (μm/h)
2	5.5	2.1	0.638
4	7.25	4.375	
6.26	10.625	7	
8	13	9.25	

Table 5.21: Determination of bulk etch rate by fission track diameter method CR-39 was exposed from ^{252}Cf, etched in 6M KOH 70 °C. ($V_B = D_f / 2t$)[41].

Etching time t(h)	Fission fragments tracks diameter D_f(μm)	α-particle tracks diameter D_α (μm)	V_B = (μm/h)
2	5.56	3	0.833
4	10	5.5	
6	12	8.5	
8	16	11.5	

Table 5.22: Effect of absorbed water on V_B, before exposure from ^{252}Cf, CR-39 was dipped in distilled water for 24 h, etched in 6M NaOH at 70 °C.

Etching time t(h)	Fission fragments tracks diameter D_f (μm)	α-particle tracks diameter D_α (μm)	V_B = (μm/h)
2	6.25	2	0.728
4	9.5	4.35	
6.083	12.5	7	
8	15	8.5	

Table 5.23: Effect of absorbed water on V_B , before exposure from ^{252}Cf, CR-39 was dipped in distilled water for 24 h, etched in 6M KOH at 70 °C.

Etching time t(h)	Fission fragments tracks diameter D_f(μm)	α-particle tracks diameter D_α (μm)	V_B = (μm/h)
2	6	3	0.925
4	9	5	
6	13	7.5	
8	17	11	

Table 5.24: Data for γ-rays dosimetry.

S.No.	Absorbed dose (Krad)	Exposure time (h)	Bulk etch rate (μ m/h)
1	1	0.23	1.058
2	5	1.13	1.175
3	10	2.25	1.276
4	20	4.50	1.736
5	30	6.75	1.974
6	40	9.00	2.250
7	50	11.25	2.593
8	60	13.50	2.946
9	100	22.50	3.396
10	200	45.00	4.814
11	300	67.50	5.1726
12	400	90.00	5.632
13	500	117.00	6.376

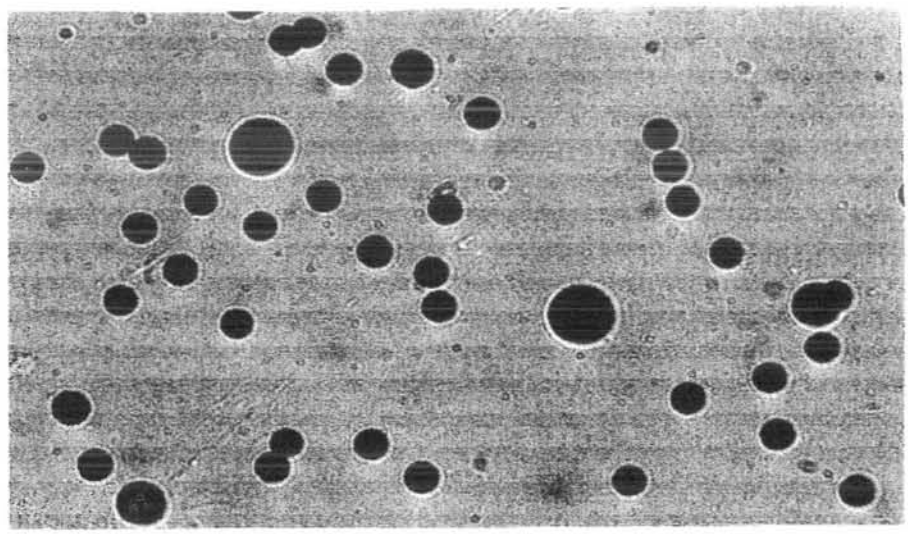

Fig. 5.1: Photograph of ^{252}Cf,fission fragment and α-particle tracks in CR-39. Etching was proceed in 6 M NaOH at 70°C for 8 hours. The tracks that have greater diameter represented the fission fragment tracks whereas small track diameter due to al-particles from ^{252}Cf.

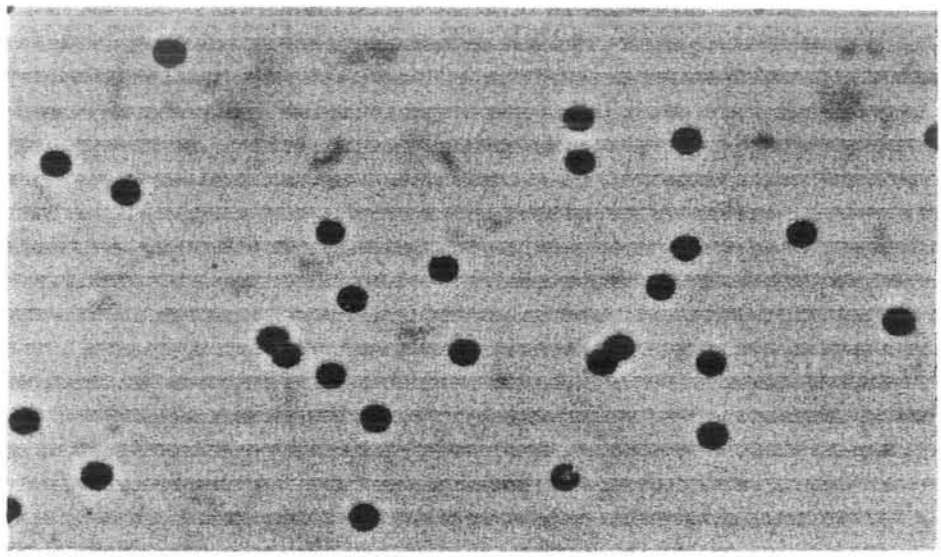

Fig. 5.2: Photography of ^{241}Am al-particle tracks in Cr-39. Etching was proceed in 6 M NaOH at 70°C for 8 hours.

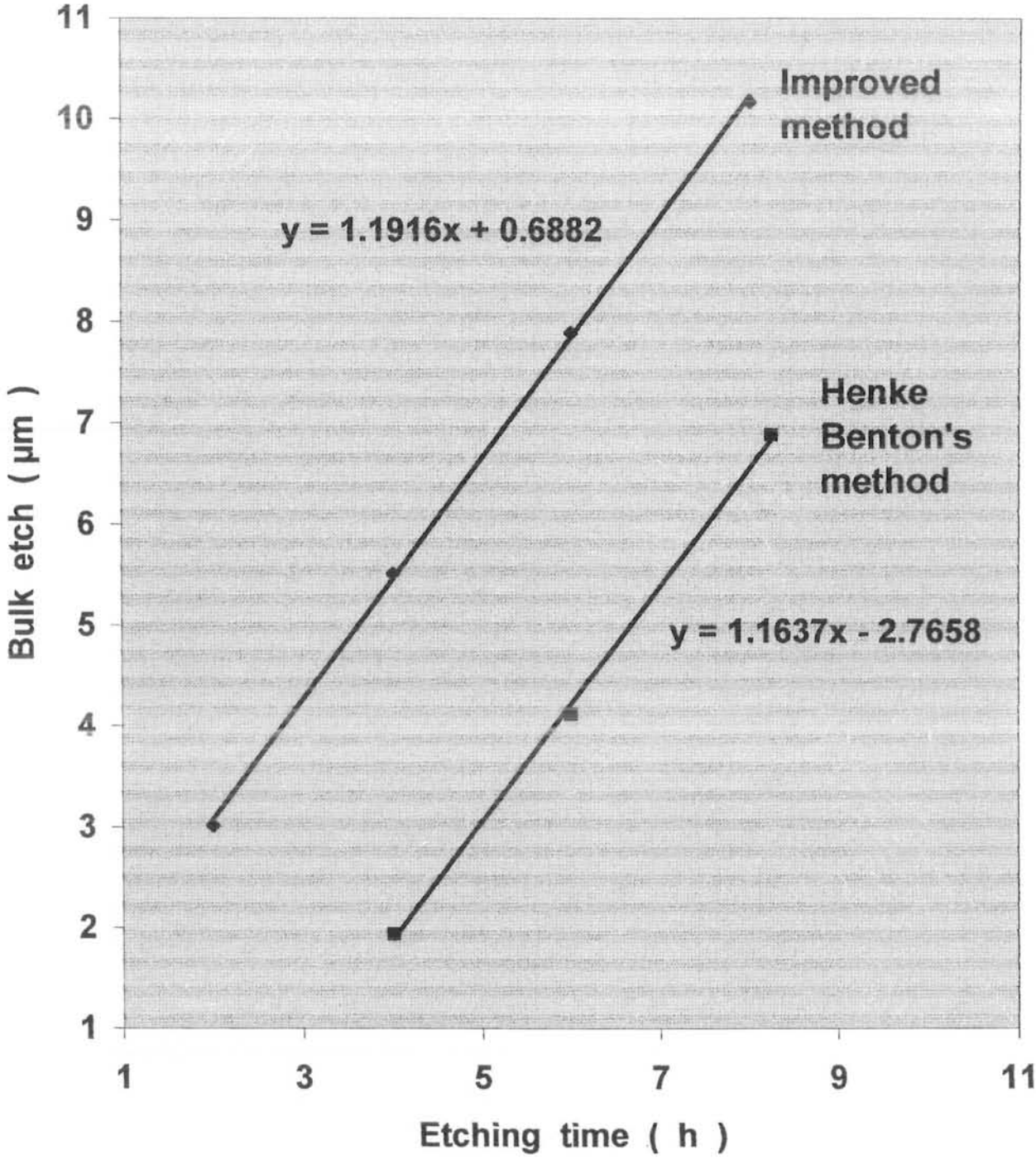

Fig. 5.3 Comparison between Henke Benton's method and improved method for bulk etch rate of CR-39 . Whereas CR-39 were etched in 6 M NaON at 70 °C .

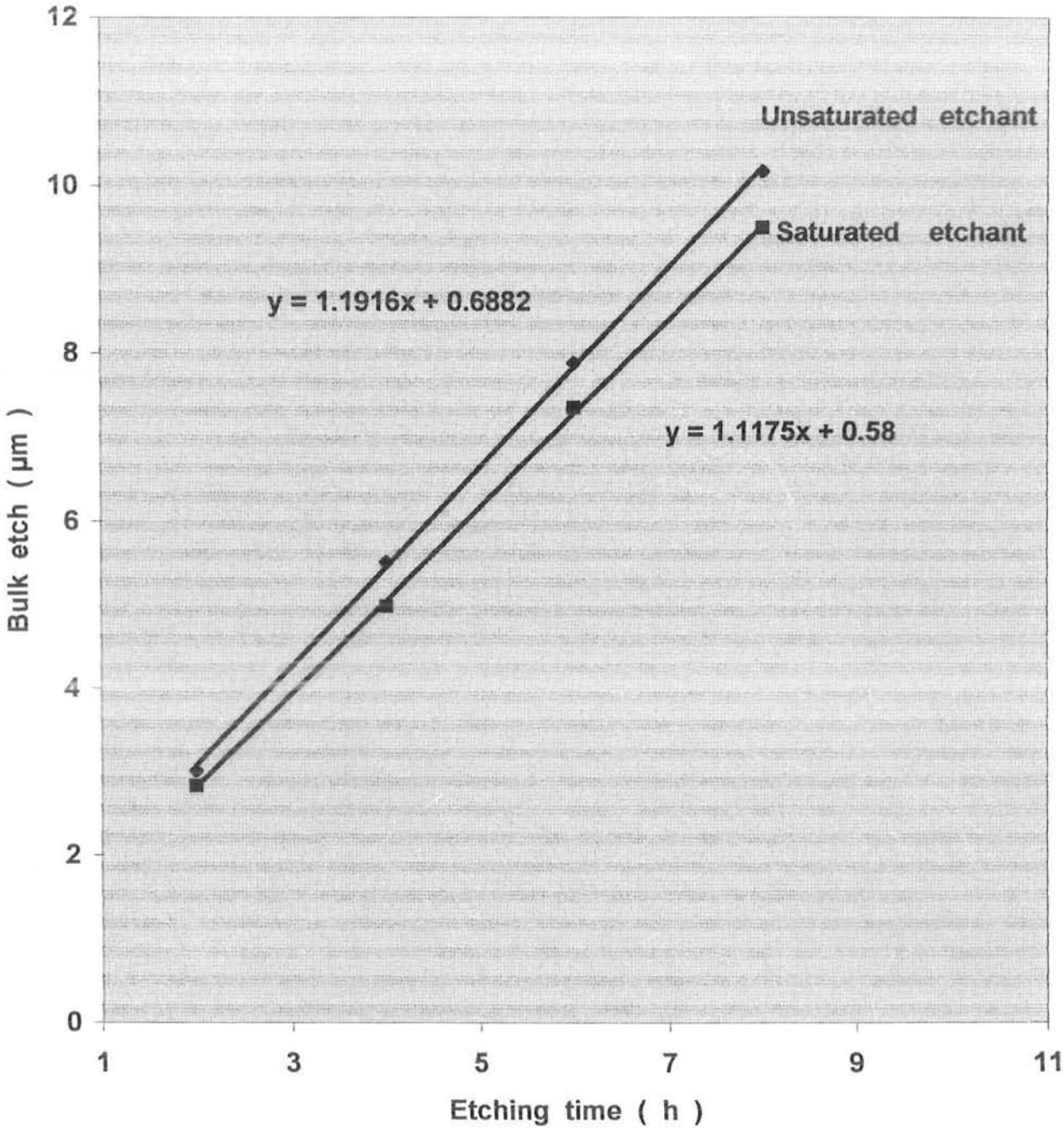

Fig . 5.4 The effect of saturated etchant on bulk etch rate . CR-39 was exposed from ^{241}Am ,etched in 6 M NaOH at 70 °C .

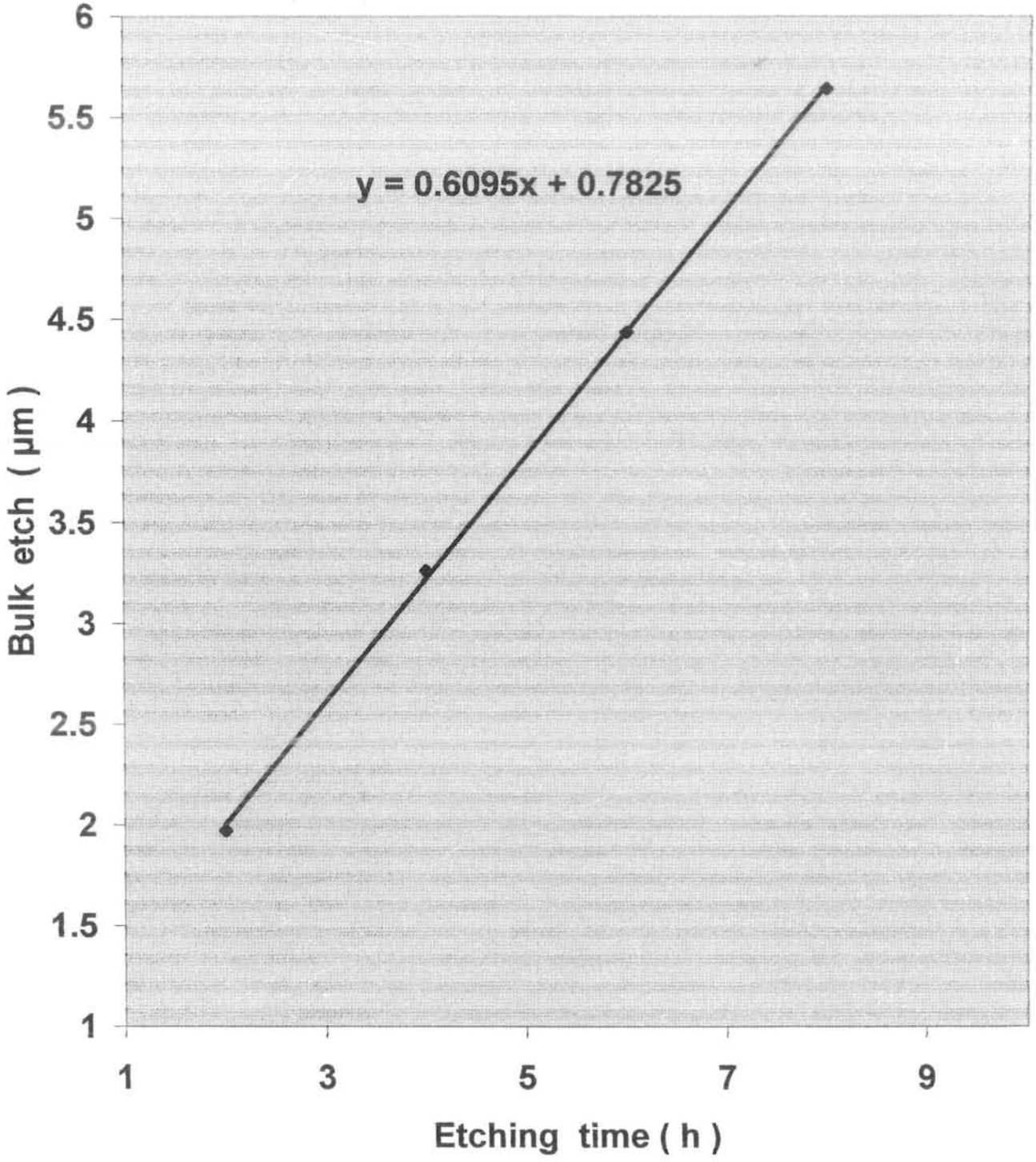

Fig .5.5 Bulk etch rate of CR-39 , exposed from ^{241}Am , etched in 4 M NaOH at 70 ^{o}C .

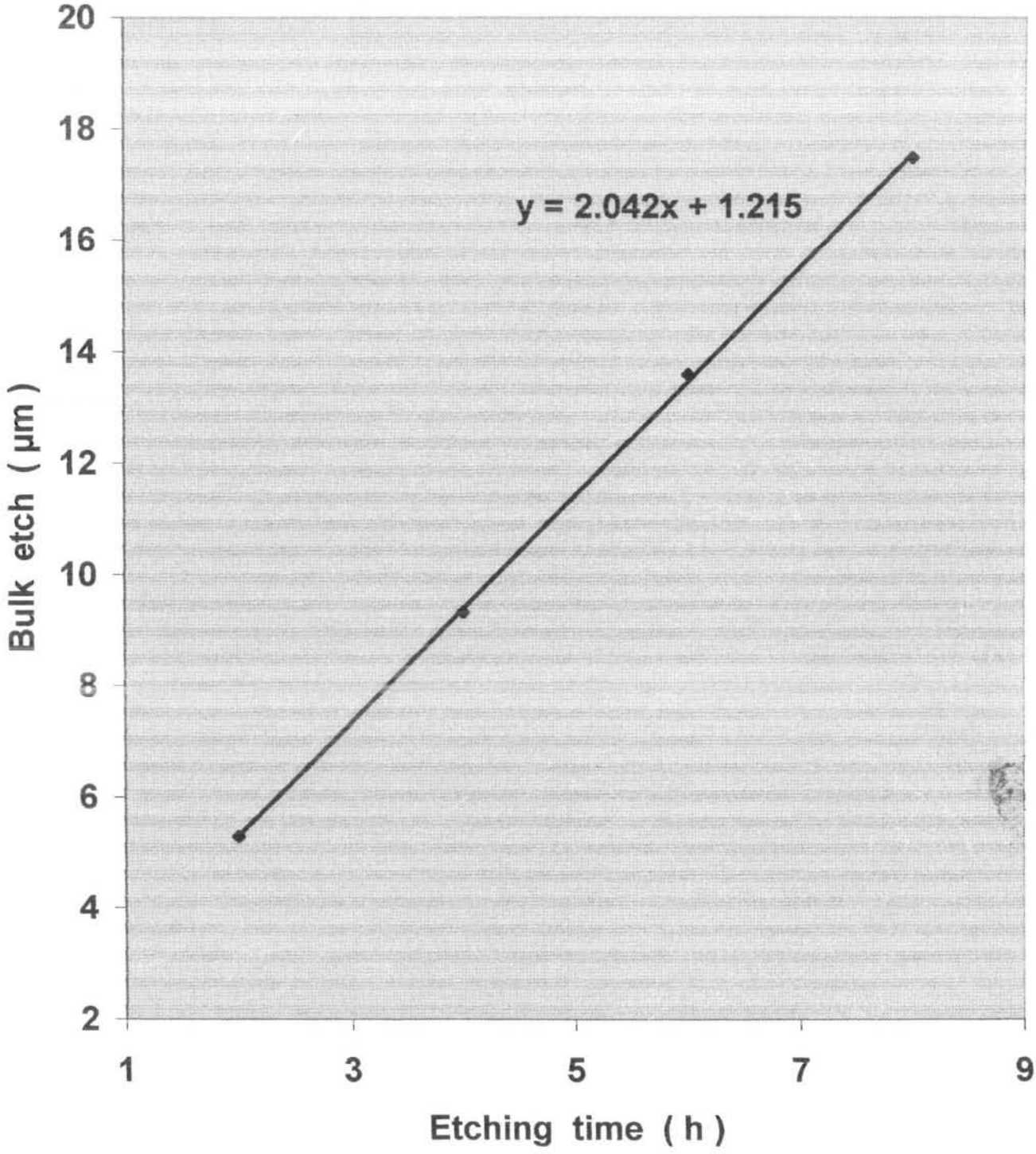

Fig . 5.6 Bulk etch rate of CR-39 , exposed from ^{241}Am , etched in 8 M NaOH at 70 ° C .

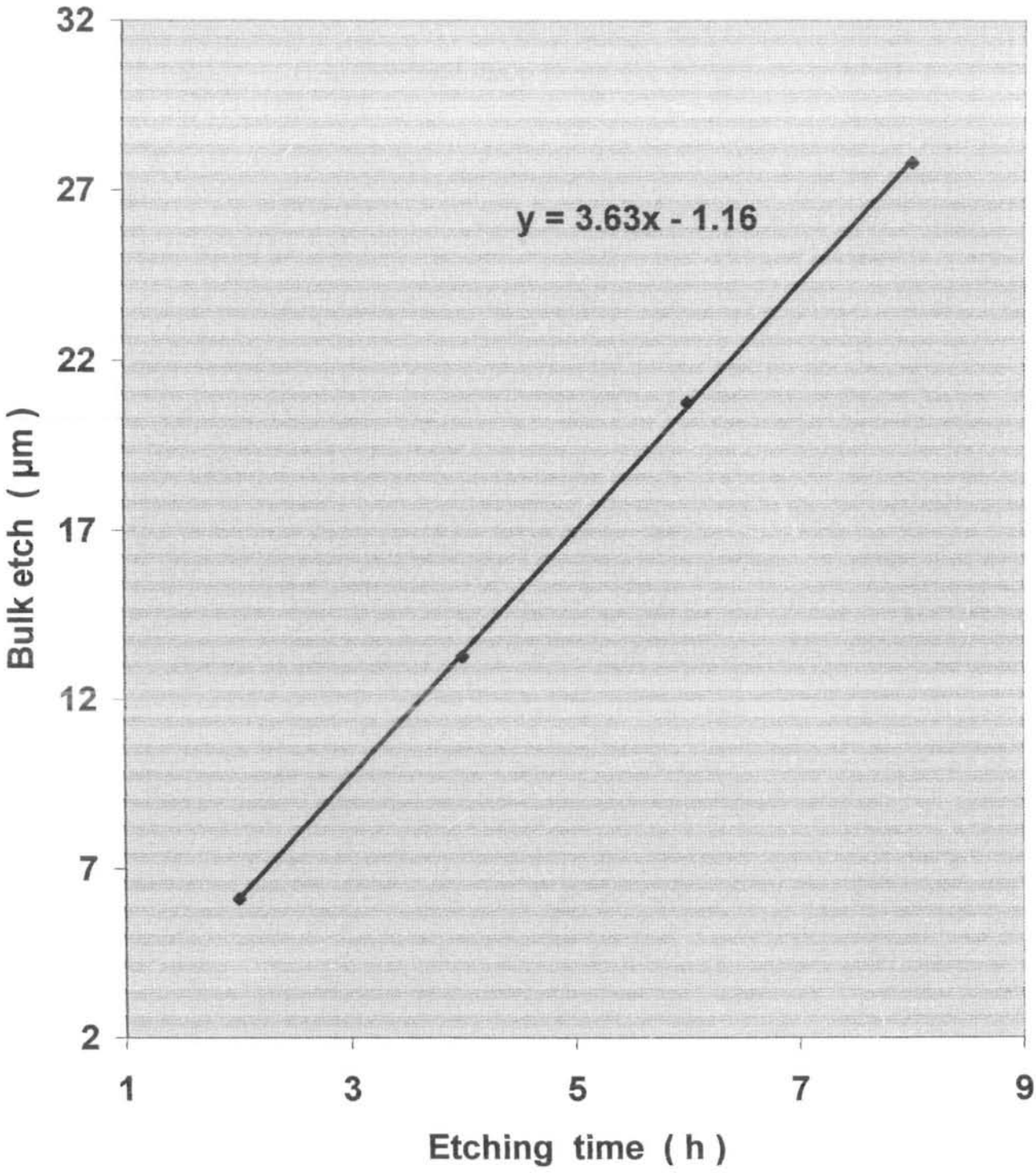

Fig . 5.7 Bulk etch rate of CR-39 , exposed from ^{241}Am , etched in 10 M NaOH at 70 °C .

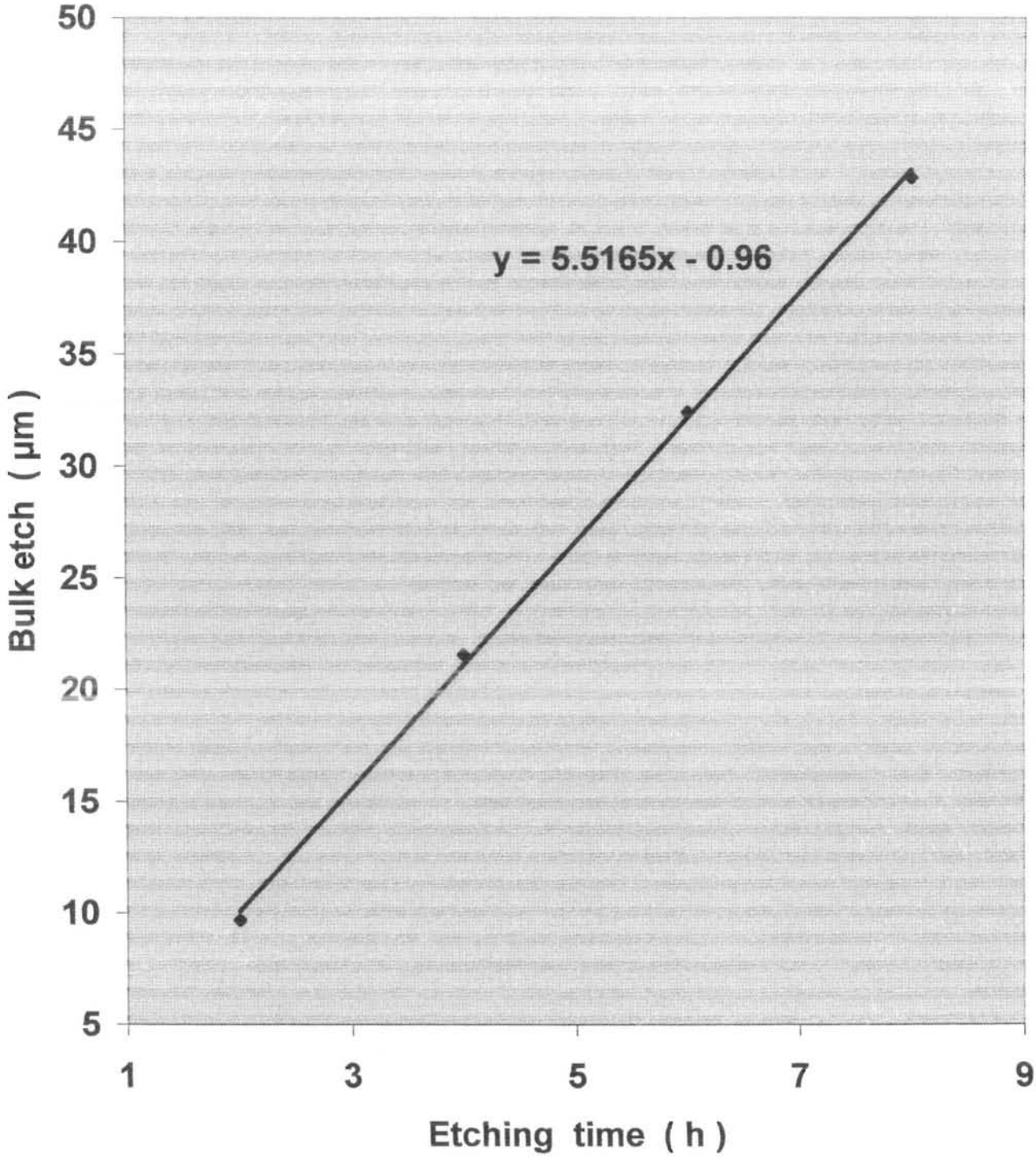

Fig . 5.8 Bulk etch rate of CR-39 , exposed from ^{241}Am , etched in 12 M NaOH at 70 °C .

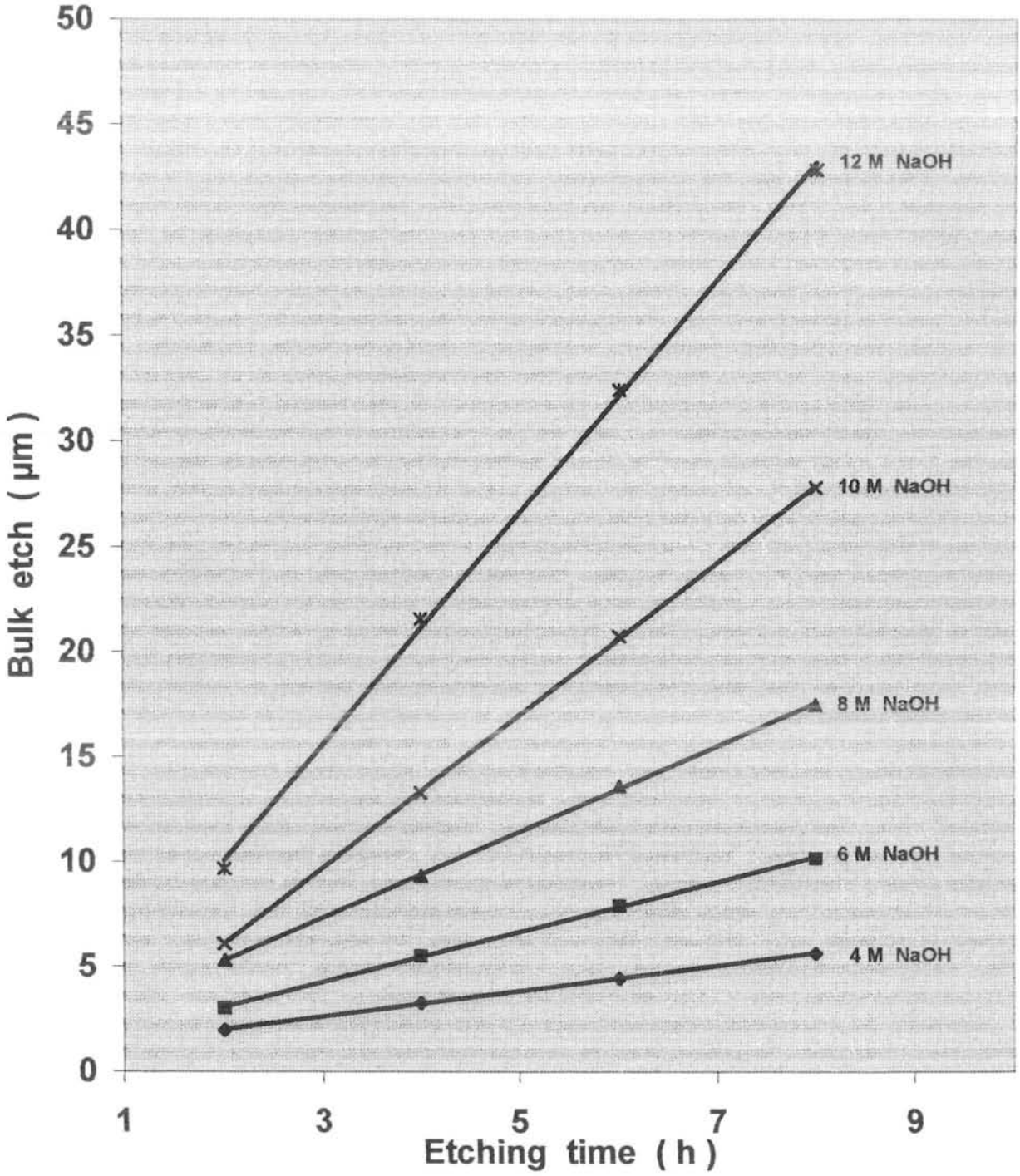

Fig . 5.9 The comparison of concentration effect on bulk etch rate of CR-39 , exposed from ^{241}Am , etching was proceed at 70 ° C .

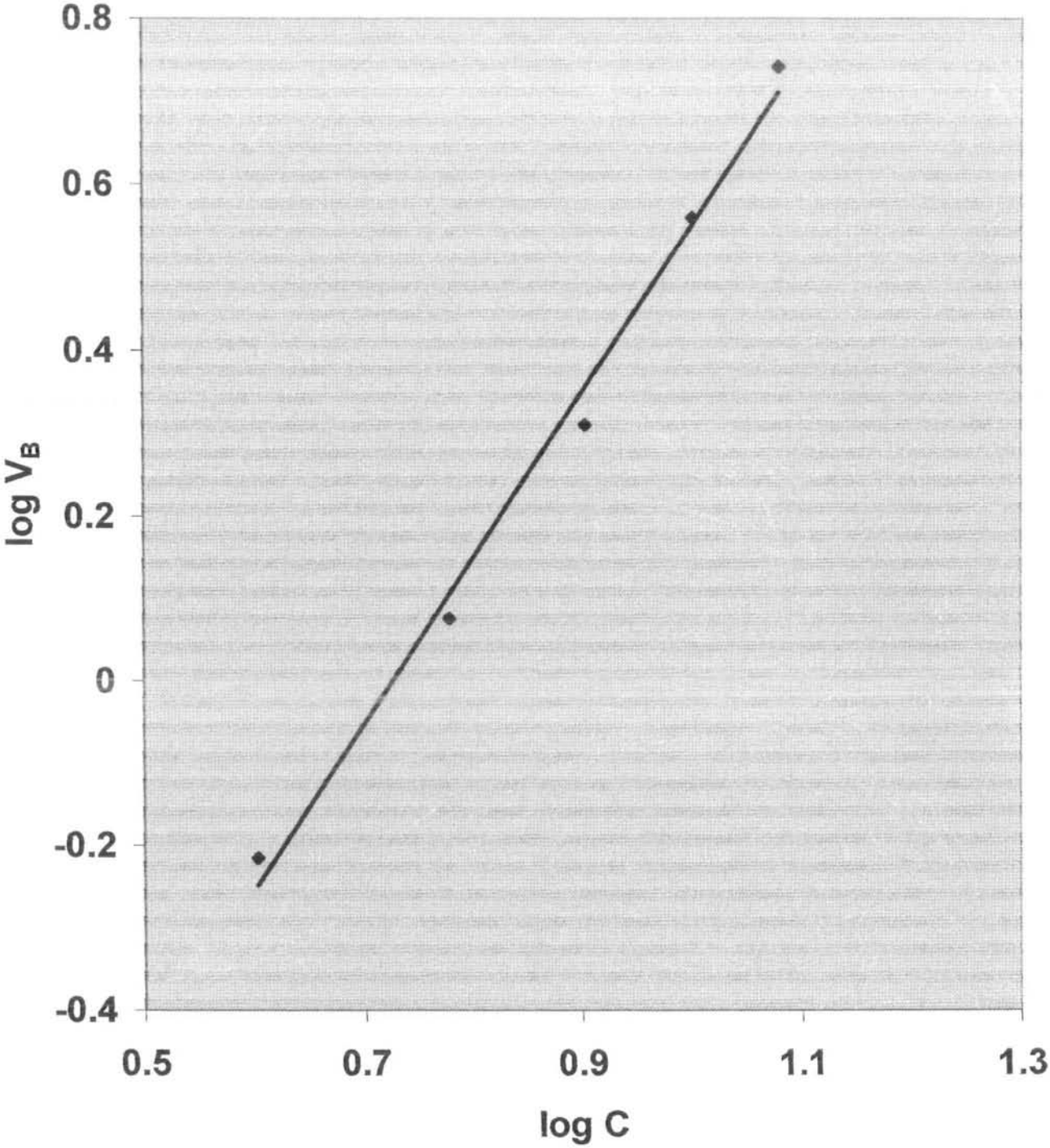

Fig .5.10 Plot of log V_B vs log C for CR-39 , shows dependence of V_B on etchant concentration .

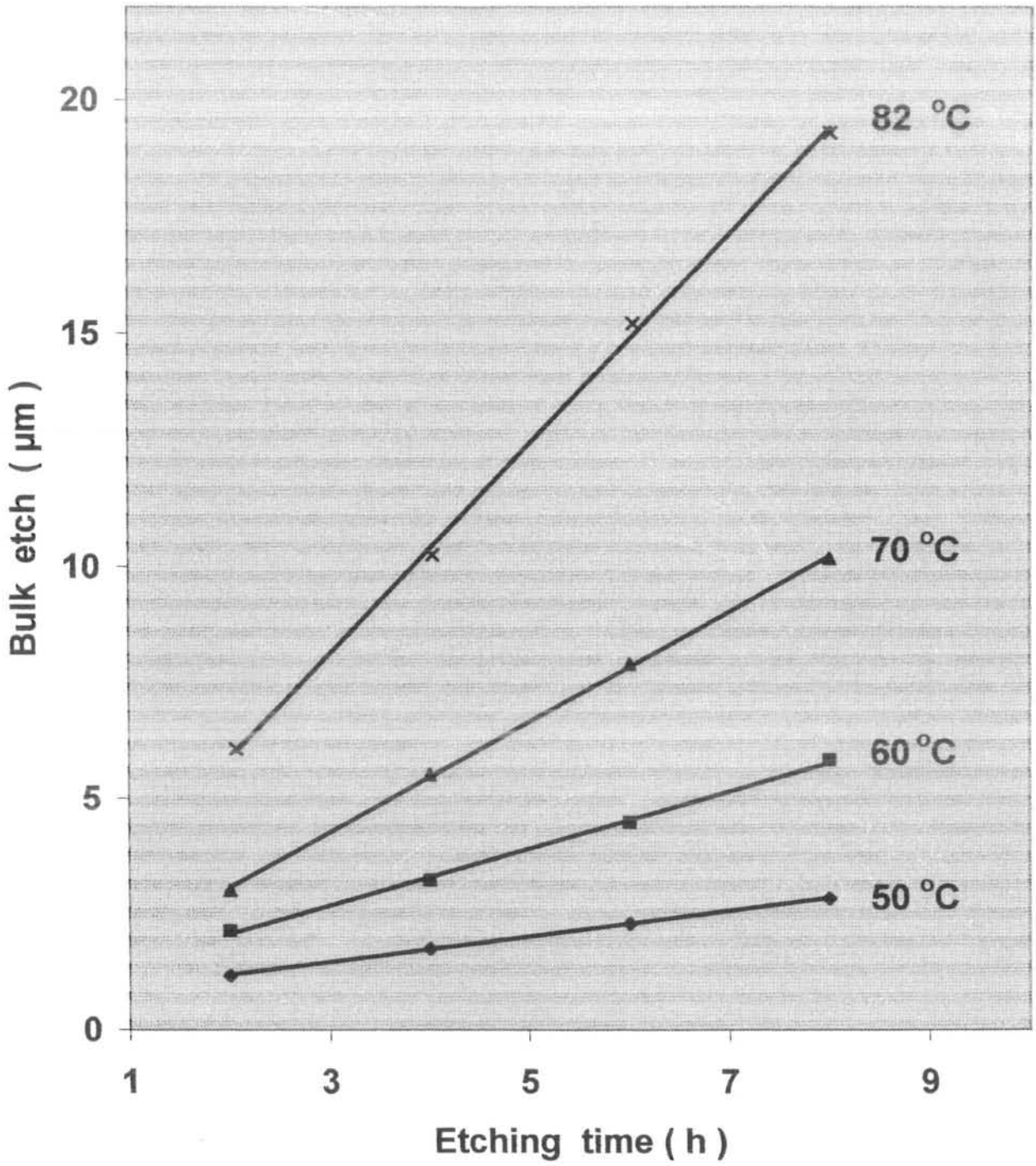

Fig .5. 11 The comparison of temperature effect on bulk etch rate of CR-39 ,etching in 6 M NaOH .

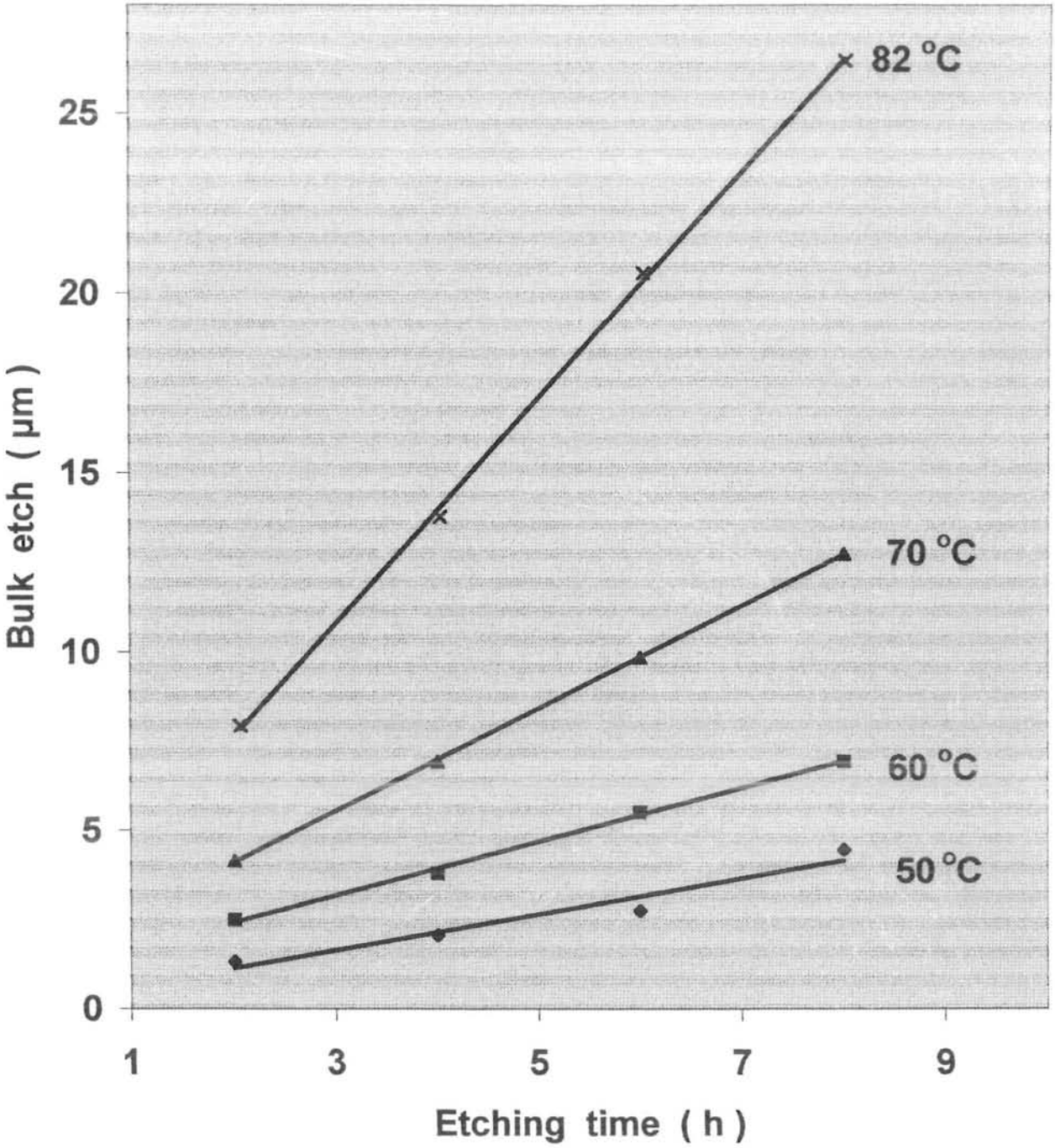

Fig . 5.12 The comparison of temperature effect on bulk etch rate of CR-39 , etching in 6 M KOH .

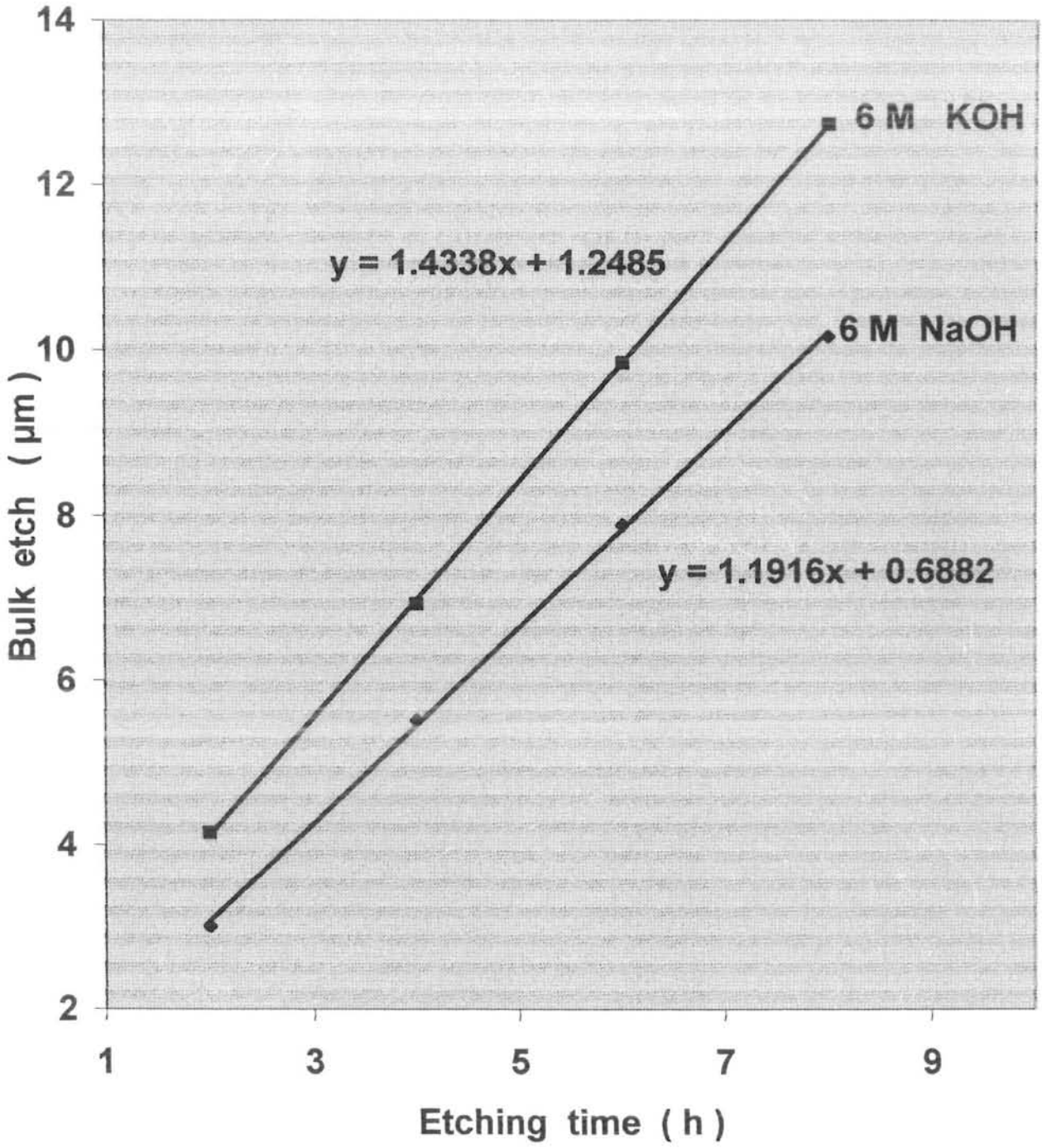

Fig . 5.13 The effect of different etchant on bulk etch rate of CR-39 , etching was proceed at 70 °C .

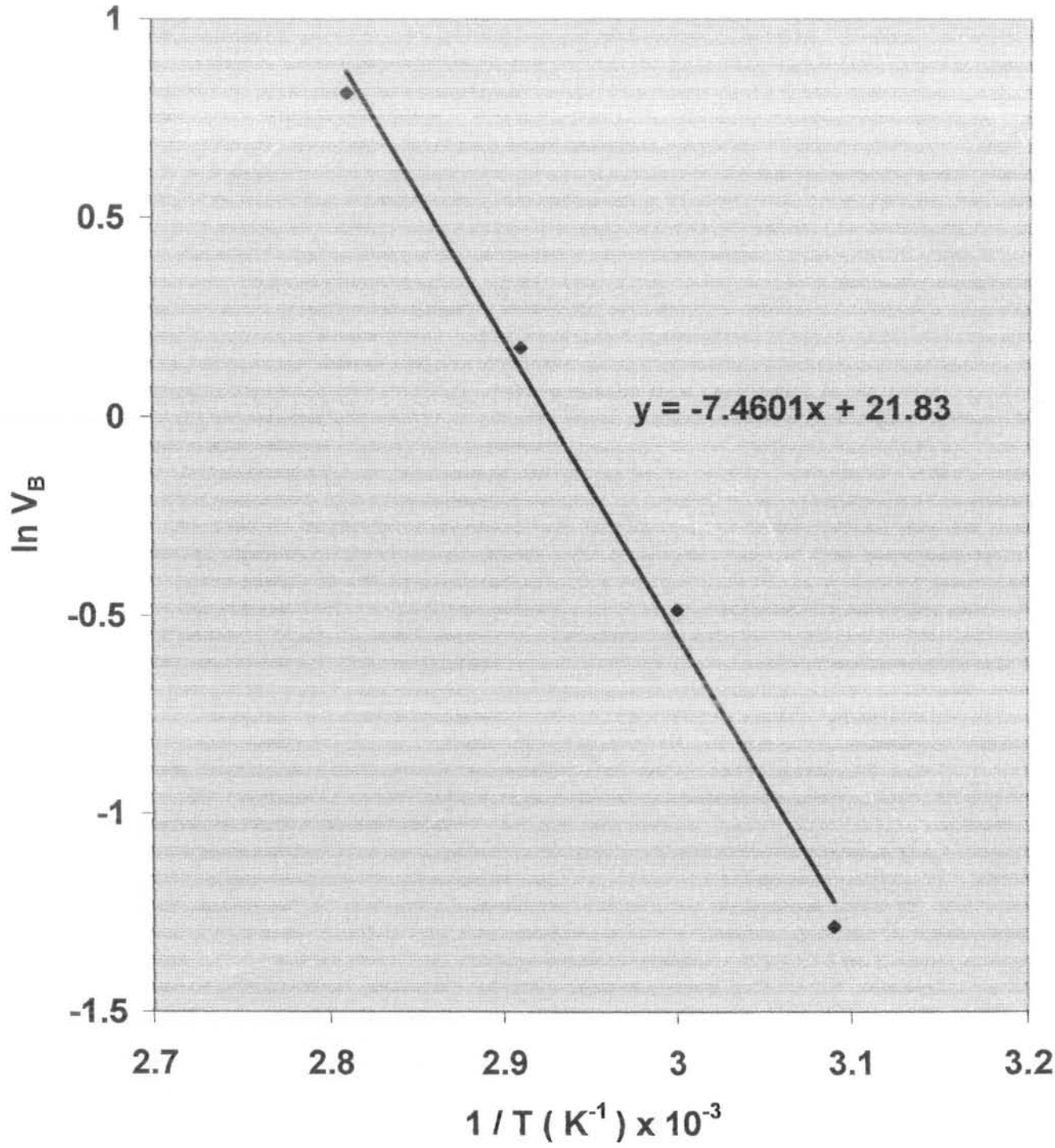

Fig . 5.14 Activation energy for bulk etching process of CR-39 ,etching in 6 M NaOH .

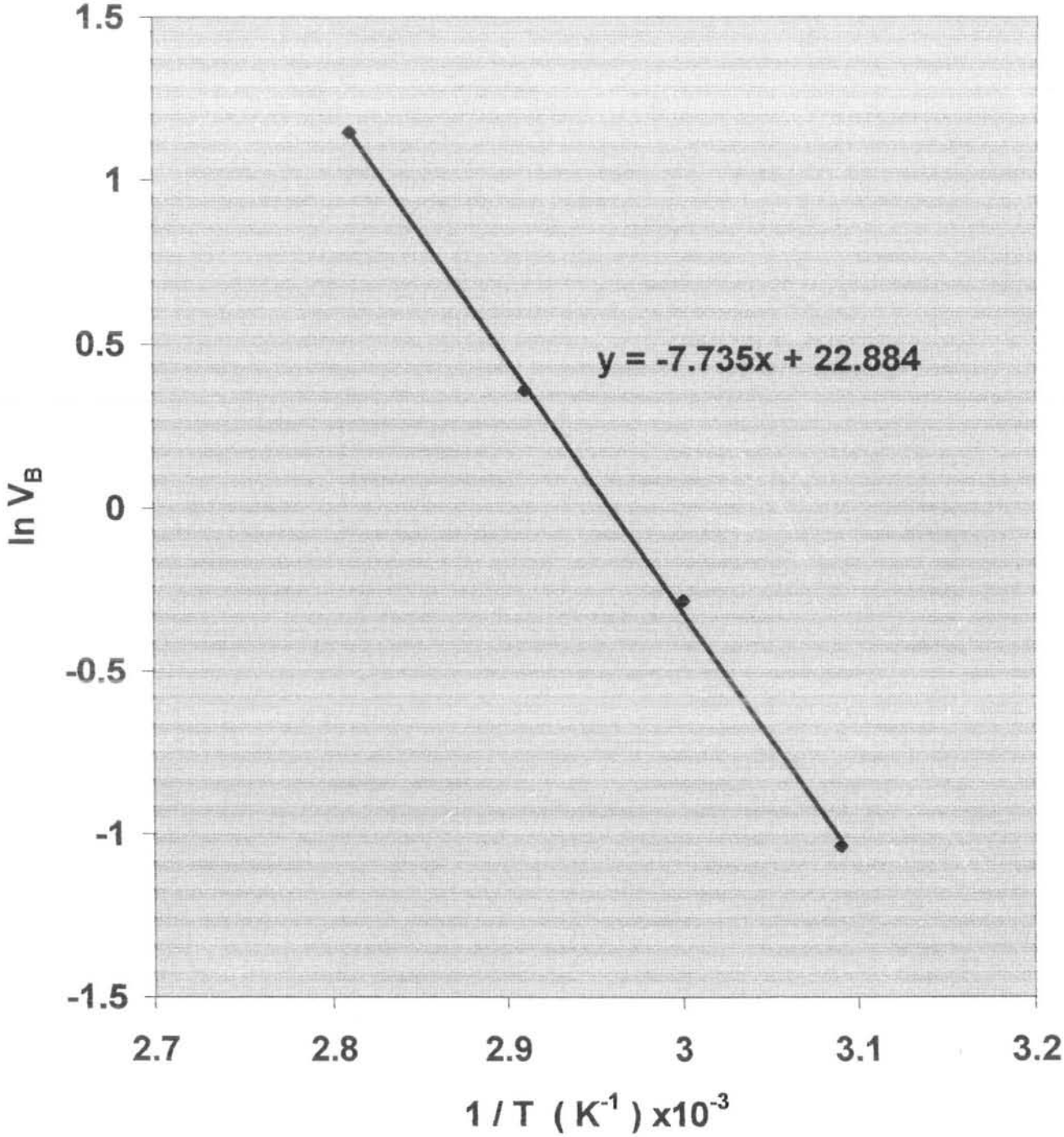

Fig . 5.15 Activation energy for bulk etching process of CR-39 ,etching in 6 M KOH .

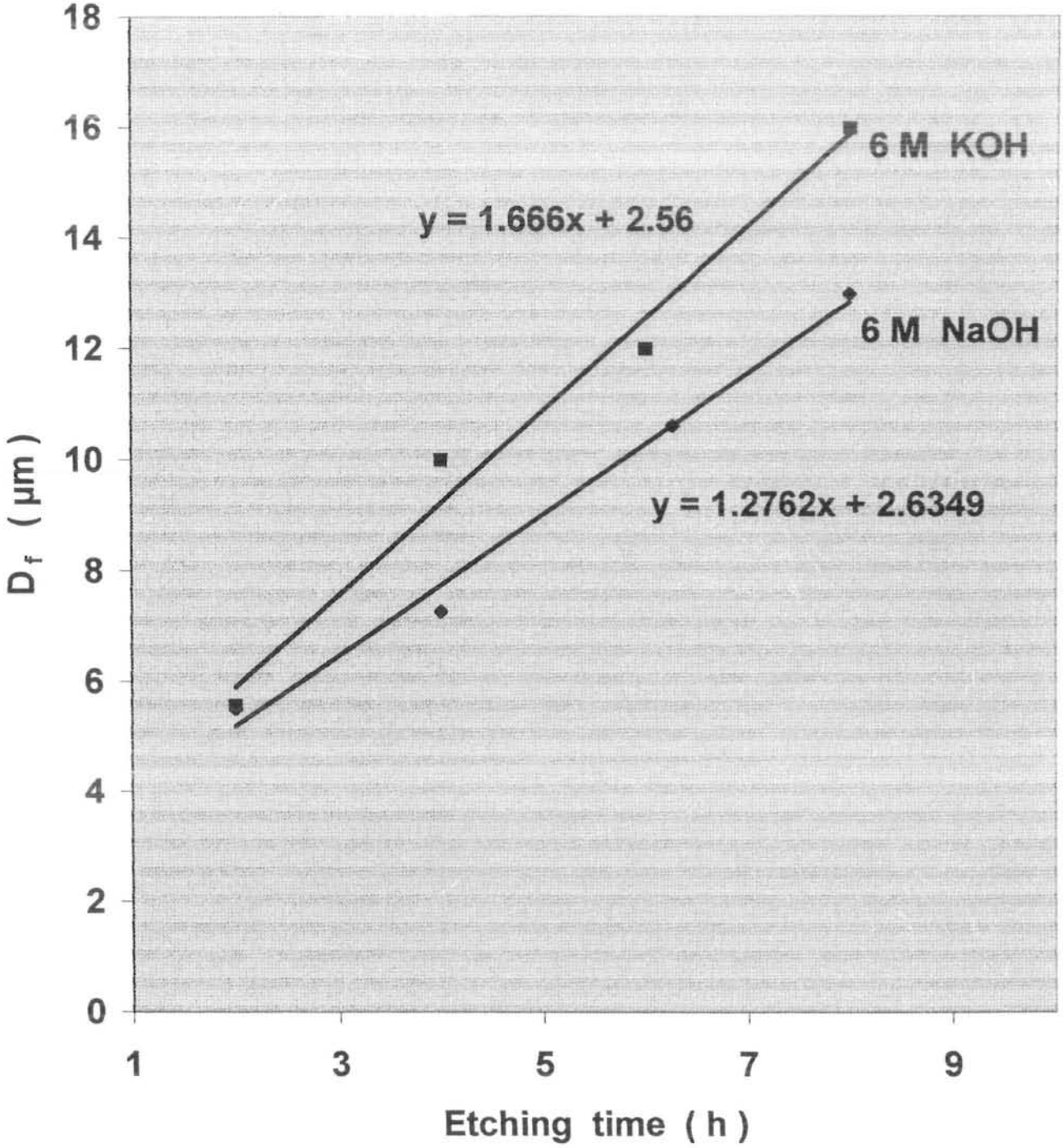

Fig . 5.16 Bulk etch rate determination by fission fragment tracks diameter method and effect of different etchant on bulk etch rate of CR-39 at 70 ^{o} C .

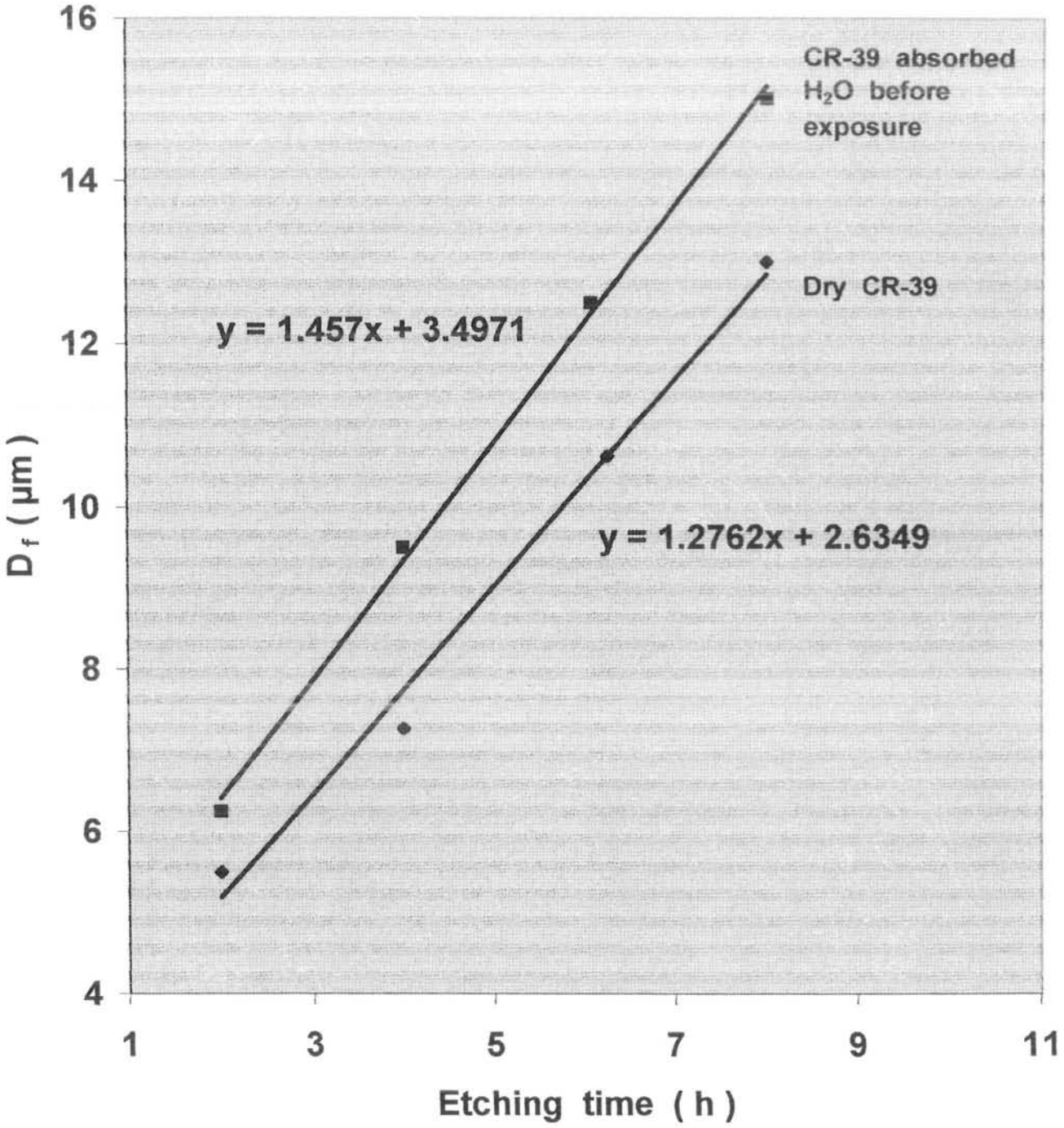

Fig . 5.17 The effect of absorbed water on bulk etch rate before exposed to CR-39 from ^{252}Cf .Whereas CR-39 were etched in 6 M NaOH at 70 ^{o} C .

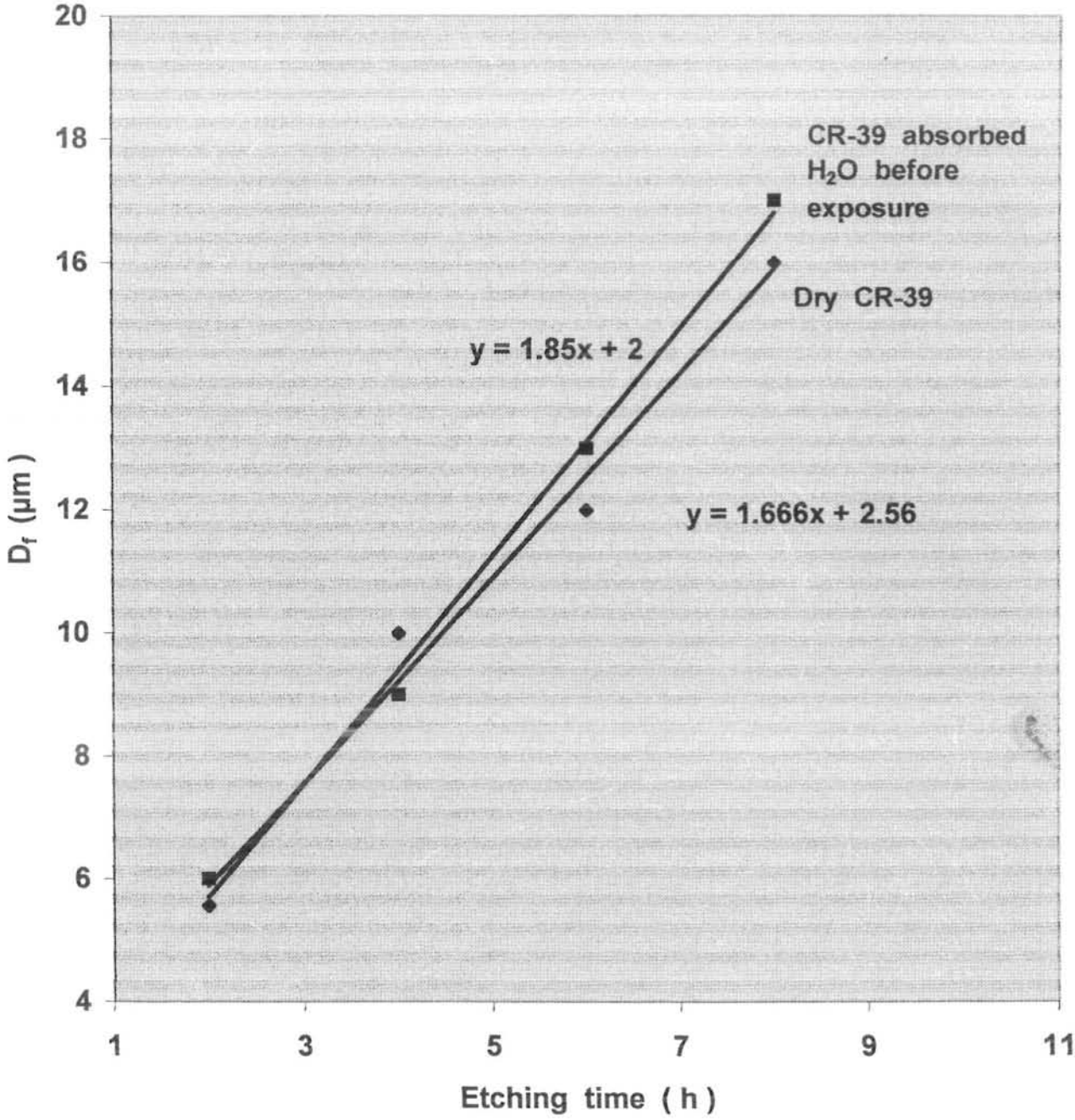

Fig . 5.18 The effect of absorbed H_2O on bulk etch rate before exposed to CR-39 from ^{252}Cf .Whereas CR-39 were etched in 6 M KOH at 70 °C .

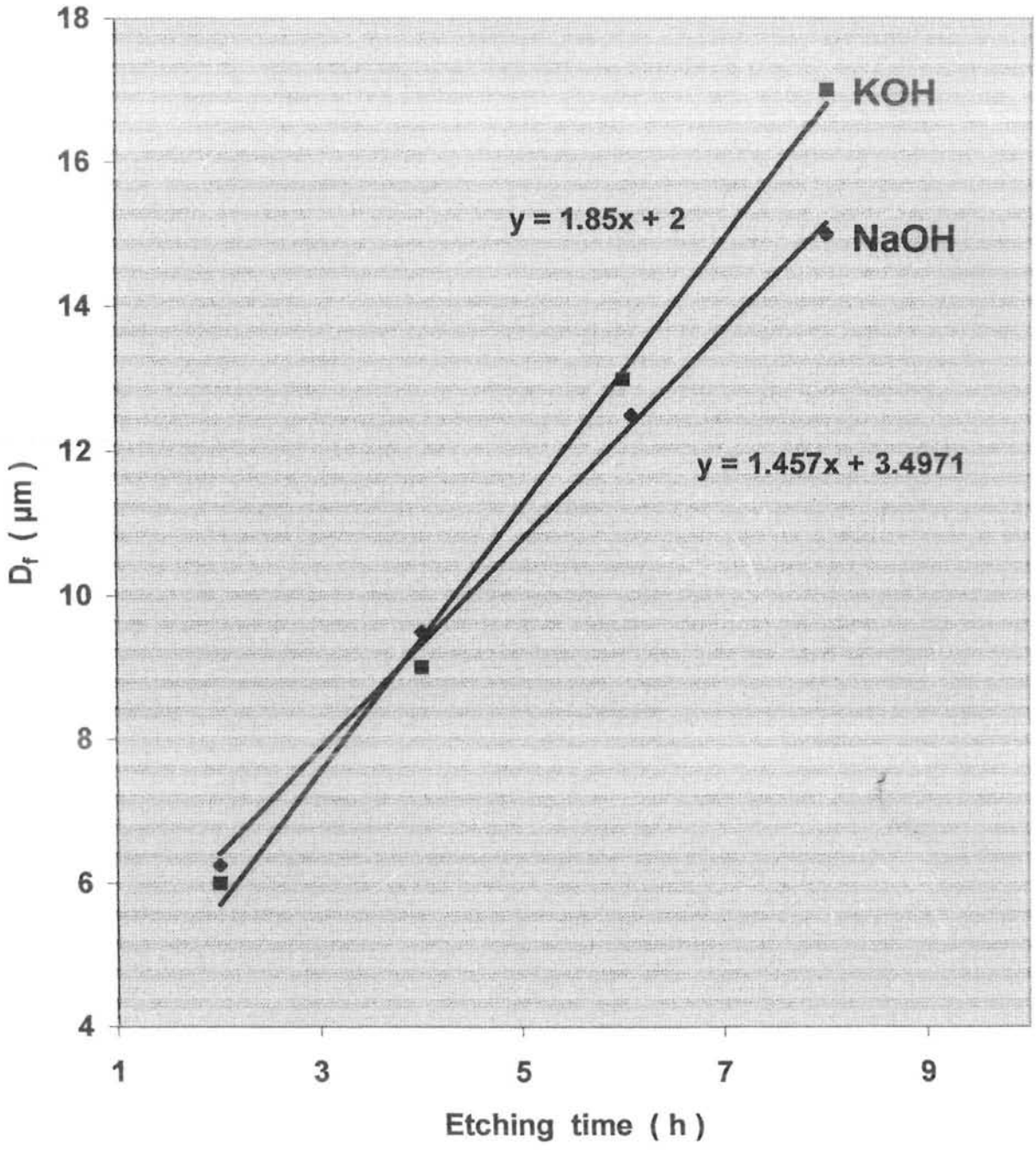

Fig .5.19 The effect of different etchant on bulk etch rate of CR-39 , etching was proceed at 70 ^{o} C . Whereas bulk etch rate was determined by fission fragment tracks diameter method .

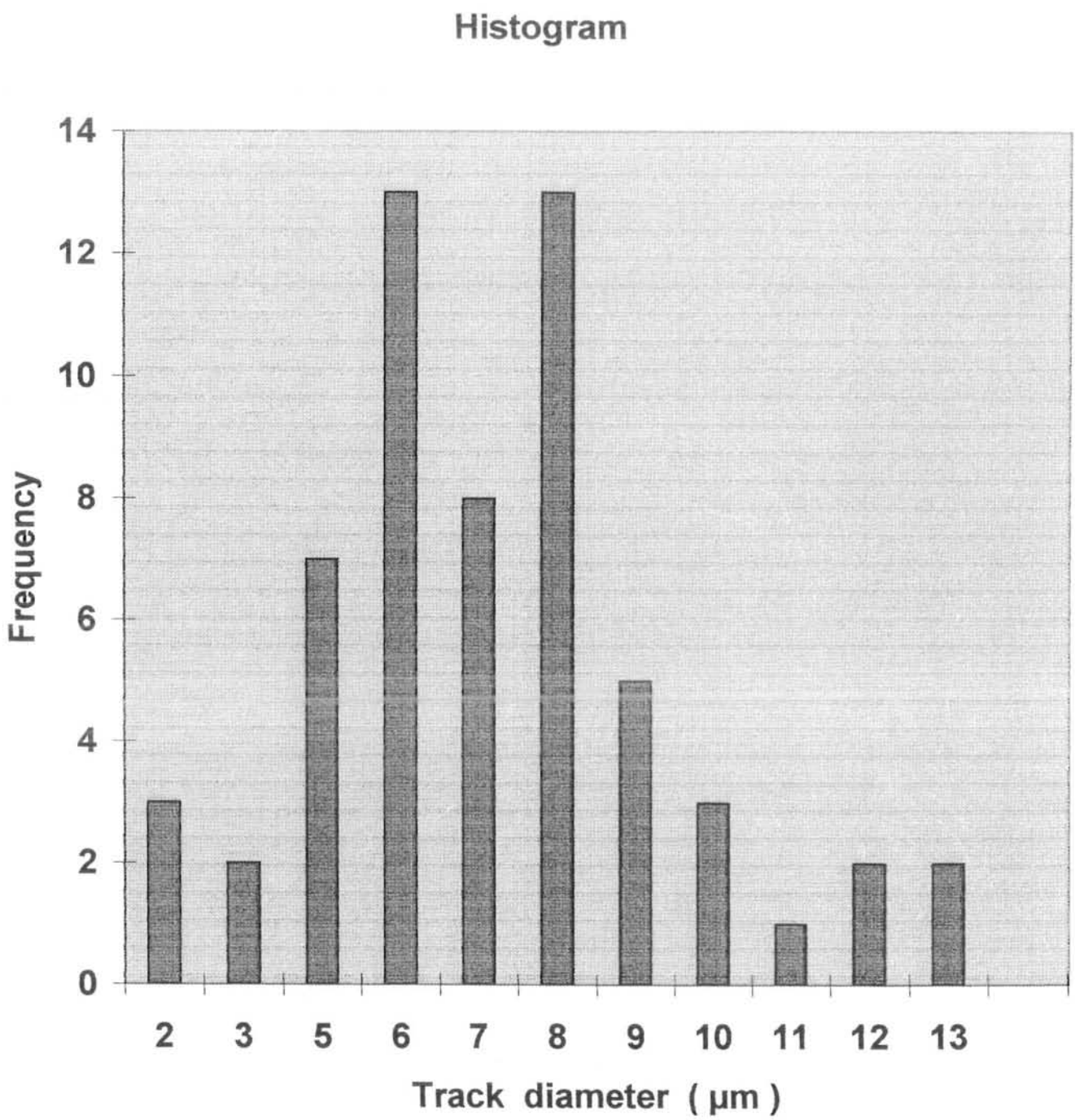

Fig .5.20 Distribution of track diameters as a function of etchant concentration . CR-39 was exposed from ^{241}Am , etched in 6M NaOH at 70 °C .

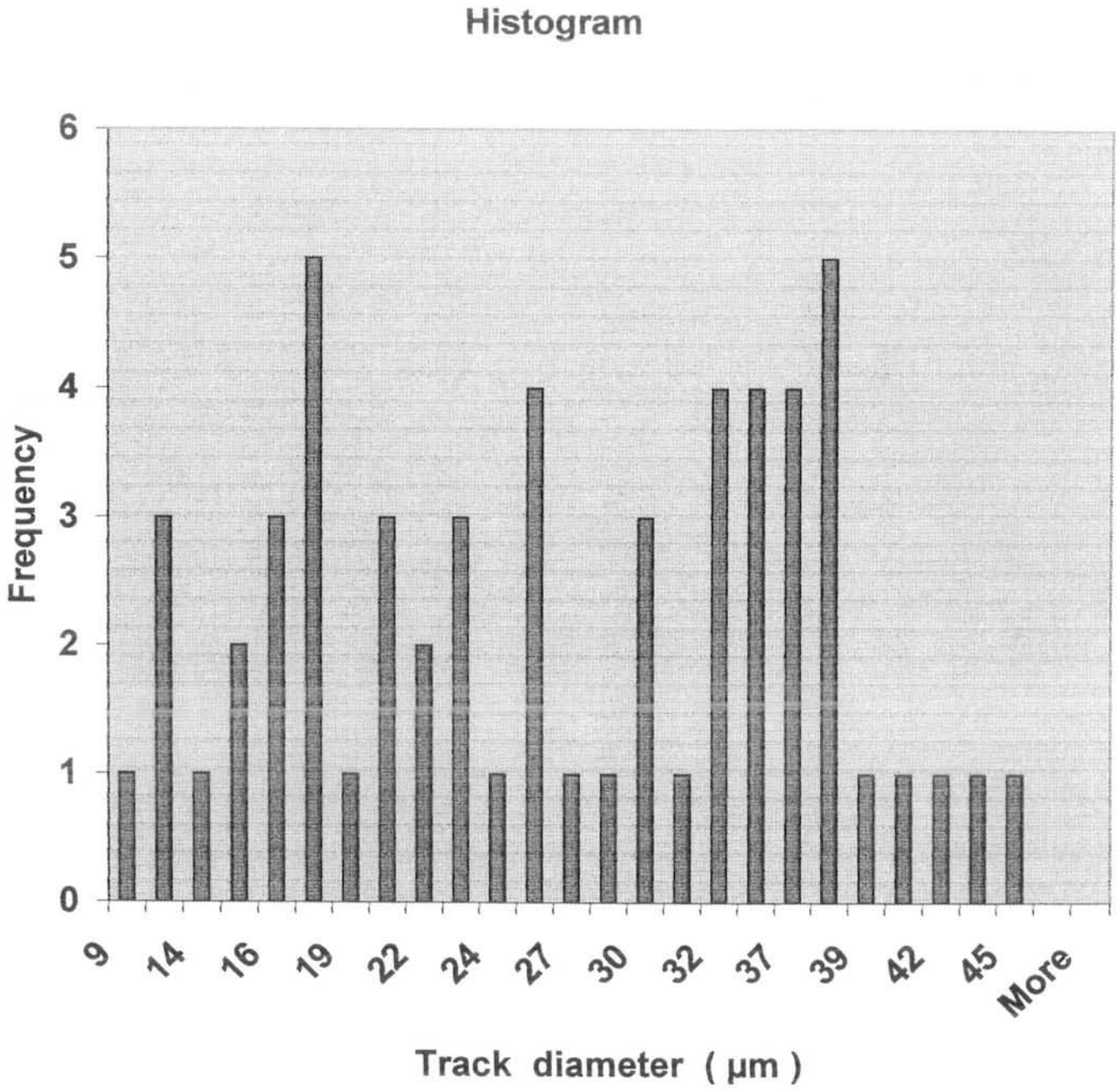

Fig .5.21 Distribution of track diameters as a function of etchant concentration . CR-39 was exposed from ^{241}Am , etched in 12 M NaOH at 70 ° C .

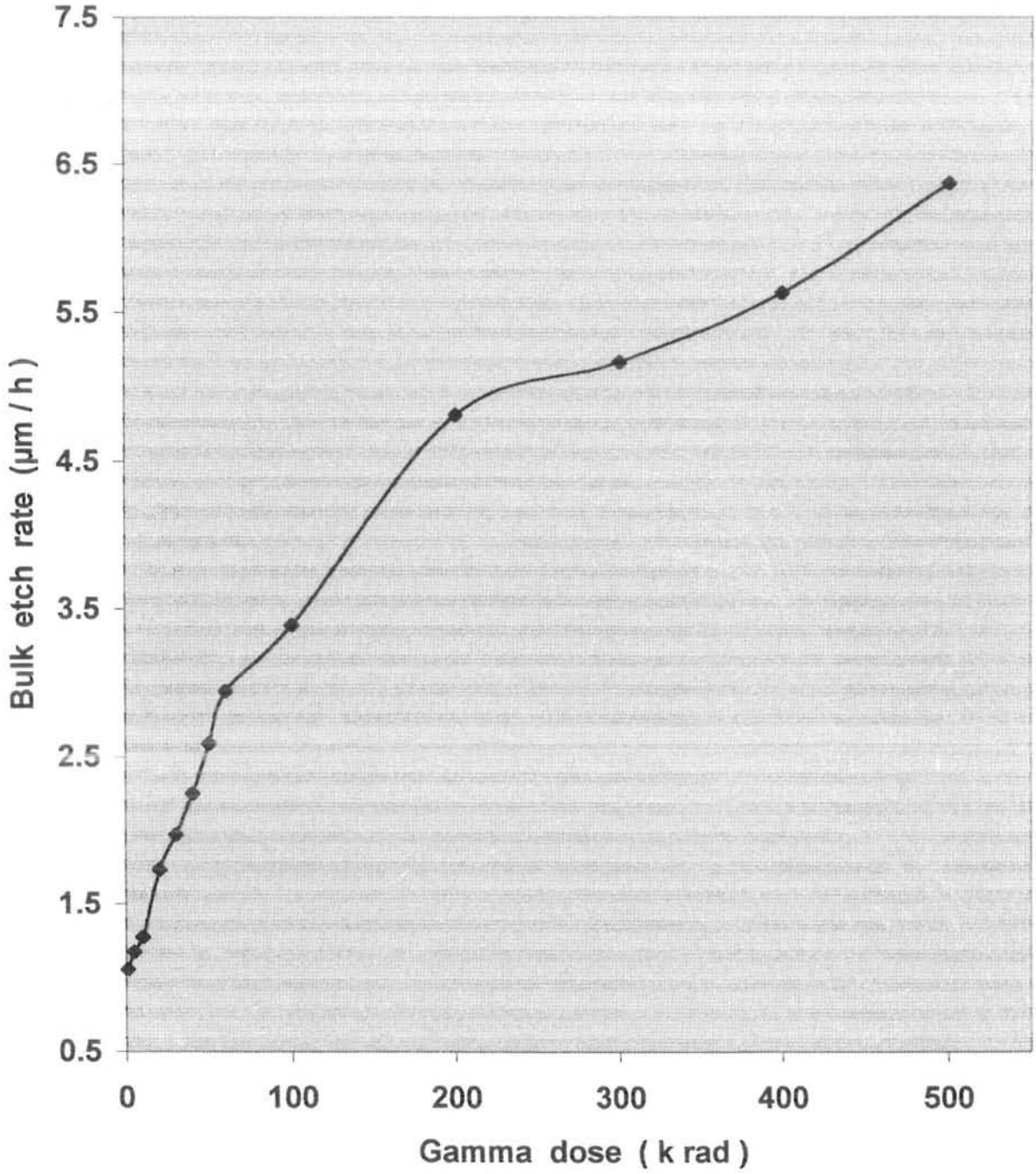

Fig . 5.22 Dependence of the bulk etch rate of CR-39 upon the absorbed dose of gamma rays .

As mentioned earlier in Section No.3.10 bulk etch rate "V_B" is being emphasized in this work and an improved method needs to be developed.

It was reported that the mass change (Henke Benton's) method provides a very consistent and reliable measurement of V_B.[39]

But Henke and Benton reported a severe problem with this method in the case of CR-39. Due to the absorption of etchant during etching, CR-39 swells causing serious systematic error in V_B measurement.[39]

In the present work we try to solve this problem and minimize the systematic error in the V_B measurement.

The absorbed etchant from CR-39 was removed by complete drying the detector.

The results obtained by using Henke Benton's method and modified method are summarized as:

(i) It is found that in mass change (Henke Benton's) method, V_B can not be calculated if the detector was etched for two hours due to the absorption of etchant (see table 5.2).

It is observed that in modified method, V_B can be calculated at any etching time (see table 5.1).

(ii) It is seen that, bulk etch "B" obtained with better and higher results by using modified method (as shown in table 5.1).

(iii) The comparison of both the methods is shown in Fig.5.3. It is found that modified method gives V_B with high accuracy and minimize the systematic error.

In an other experiment, it was observed that the prolonged use of etchant solution the etch products are formed, as a result solution becomes saturated. It is found that V_B decreased due to saturated etchant (see Fig.5.4.).

An other set of experiments the influence of changes in the etching parameters on the detector's efficiency has been studied.

A linear plot is obtained between log V_B vs log C for CR-39 detector (as shown in Fig.5.10). It indicates the dependence of V_B on etchant concentration.

Further more it is observed that KOH appear to be more efficient than NaOH for bulk etch rate of CR-39 (see Fig. 5.13). The linear plots of log V_B Vs 1/T were obtained (see Fig.5.14 and Fig.5.15). These plots indicate an exponential dependence of V_B on temperature. The activation energy for the bulk etching of CR-39 is calculated from the slopes of the respective plots. Activation energy is found to be 0.64 eV and 0.66 eV for NaOH and KOH respectively.

From these results it is concluded that the activation energy of bulk etching is fairly independent of the nature of the etchant and its parameters like concentration and temperature. It is a characteristic of the bulk material and remain constant.

It is observed that our modified method gives better results of bulk etch rate than fission fragment track diameter method (as shown in Fig.5.16) Whereas, the efficiency of KOH is in good agreement with our previous experimental results (see Fig.5.19).

It was further observed that the enhancement of V_B by the factor of 1.14 and 1.11 takes place due to absorbed water before exposure in the case of NaOH and KOH respectively.

Fig. 5.20 and 5.21 show the frequency distribution of alpha track diameters as a function of etchant concentration. Data was obtained in the case of 6M NaOH with little scatter about the mean (see Fig. 5.20), whereas in the case of 12M NaOH with large scatter about the mean (as shown in Fig. 5.21). It was fuond that the etchant concentration was effected on the alpha track diameters.

The effect of gamma rays doses up to 500 krad on the bulk etch rate of CR-39 detector has been investigated .

It has been reported[73] that the bulk etch rate strongly dependent on the dose-rate. It was observed that the dose rate was not remaining constant, in our experimental work due to the human error . (see table 5.24) Therefore it was not possible to established the clear relationship between the bulk etch rate of CR-39 and absorbed dose. However the Fig.5.22 shows a dependence of the bulk etch rate upon the gamma absorbed dose.

5.4 SUGGESTIONS FOR FURTHER WORK

In order to make another aspect of SSNTDs studies the preliminary work were carried out to investigate the UV absorbance behavior of CR-39 detector.

Different sets of CR-39 detectors of thickness 500 μm and 1 x 3 cm^2 area were exposed to an electroplated ^{241}Am alpha source. The exposed detectors were then etched in 6M NaOH solution at 70°C for different etching times. The UV-spectra of unexposed and exposed etched detectors were obtained in the range of 190 to 400 nm.

It was found that the absorbance of UV light by CR-39 strongly dependence upon the exposure to the CR-39 detector as well as etching time.

More detailed studies are need to investigate the factors responsible for UV absorbance of CR-39 detectors as a function of irradiation and etching time. Further more correlation can be obtained between the UV-spectra of exposed CR-39 and SSNTD's parameters.

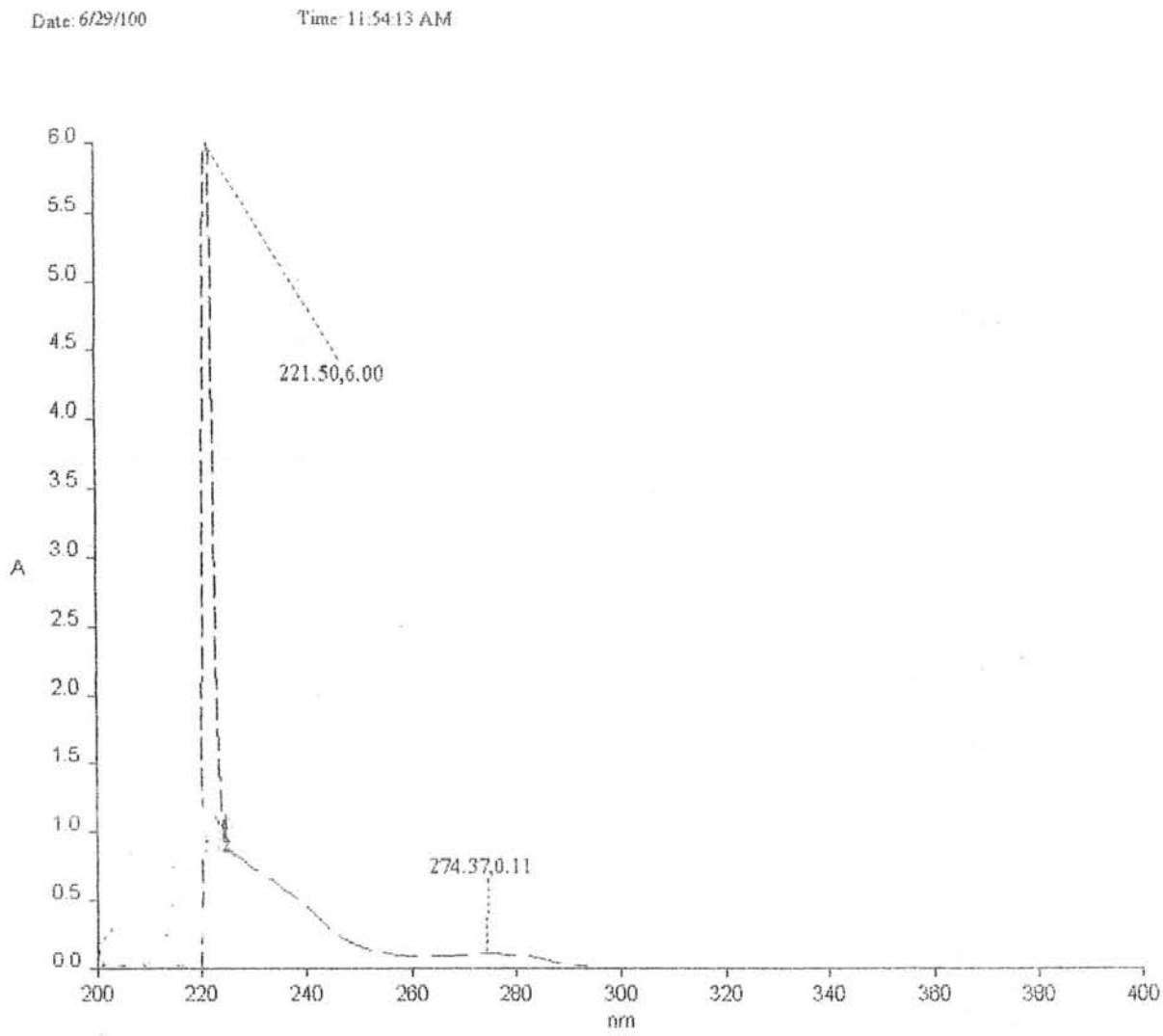

Fig.5.23 Absorption spectrum of unexposed CR-39, etched in 6M NaOH at 70 for 2 hours.

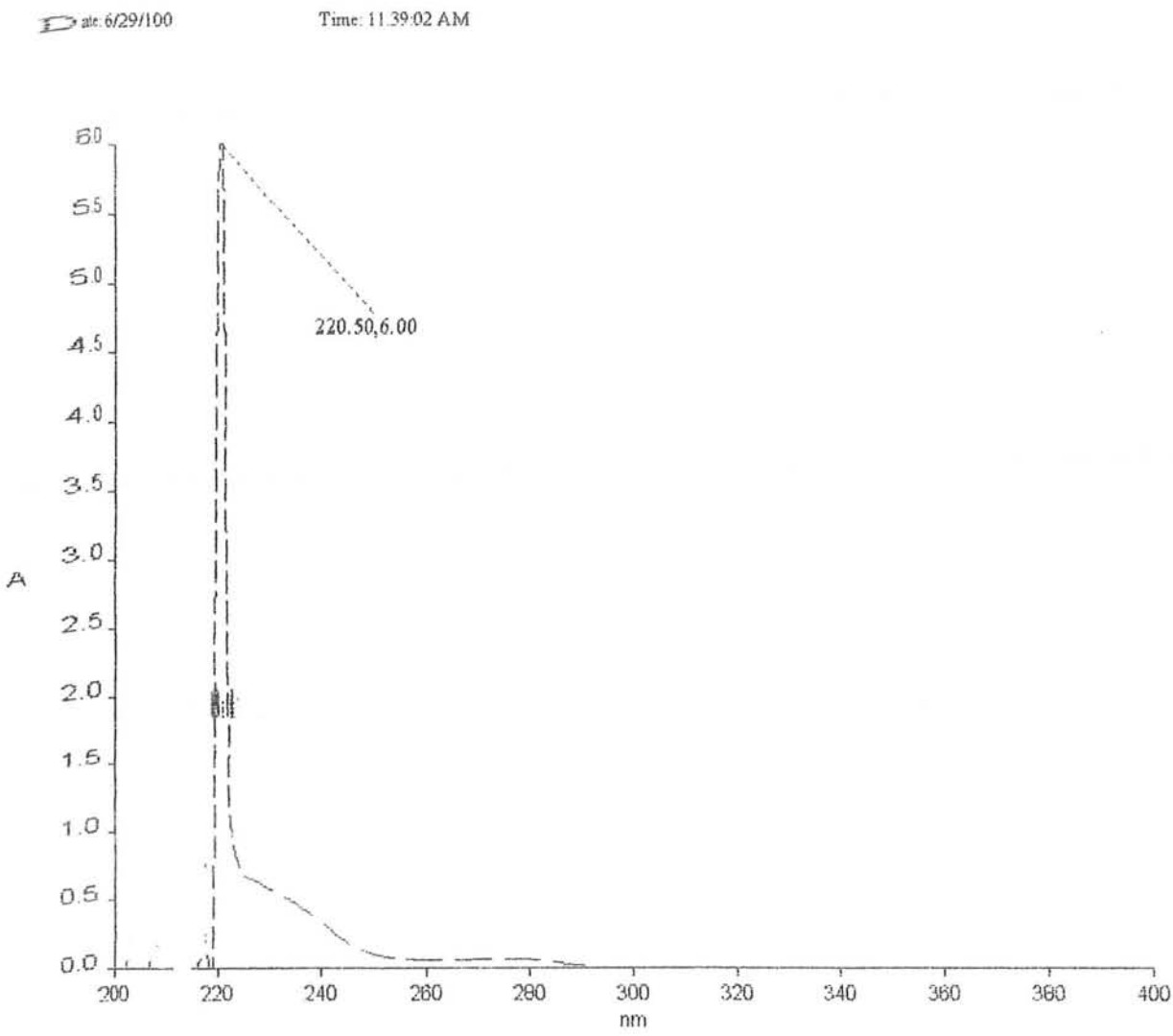

Fig.5.24 Absorption spectrum of exposed CR-39 from ^{241}Am, etched in 6M NaOH at 70 ^{o}C for 2 hours.

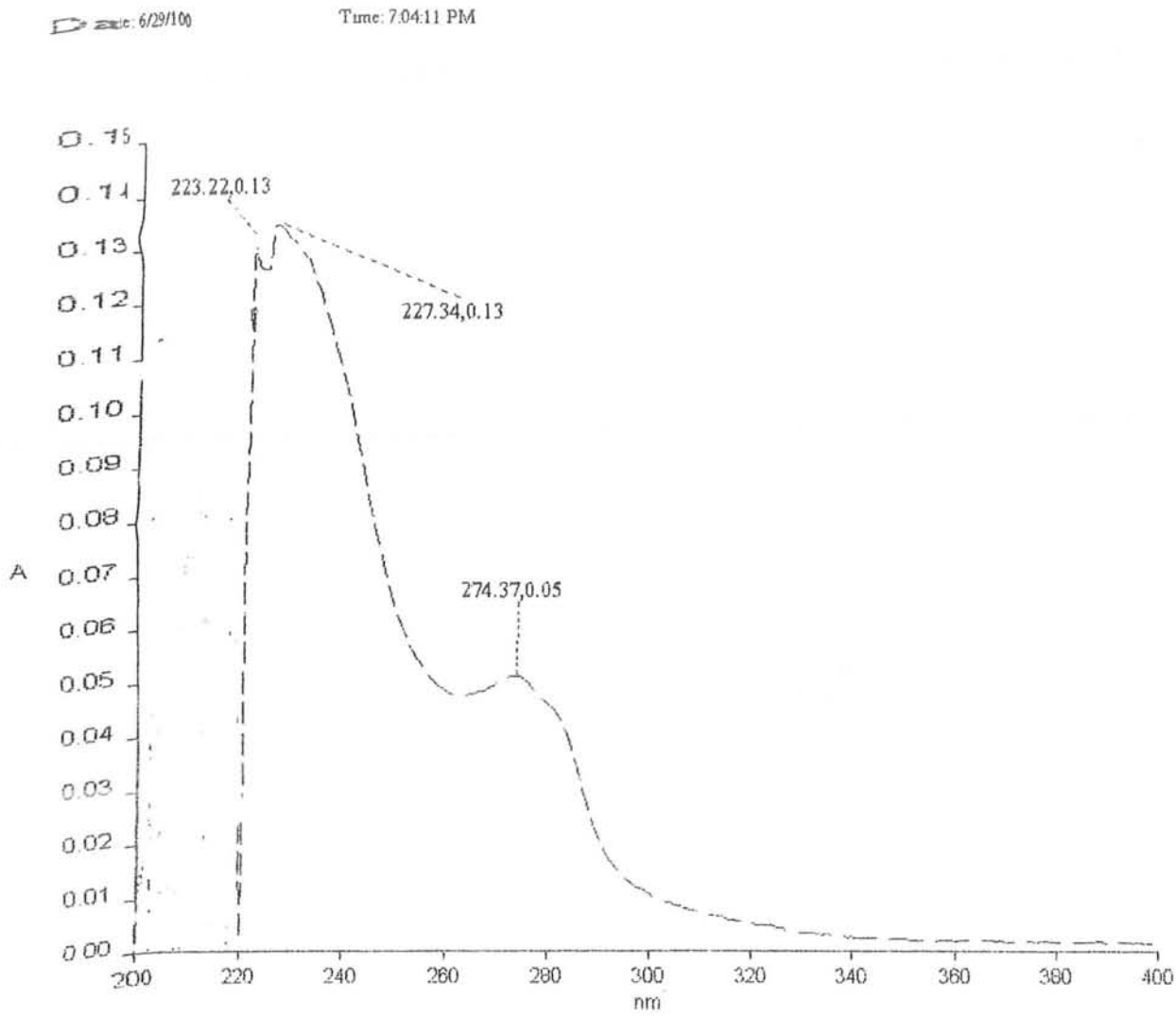

Fig.5.25 Absorption spectrum of unexposed CR-39, etched in 6M NaOH at 70 ^{o}C for 4 hours.

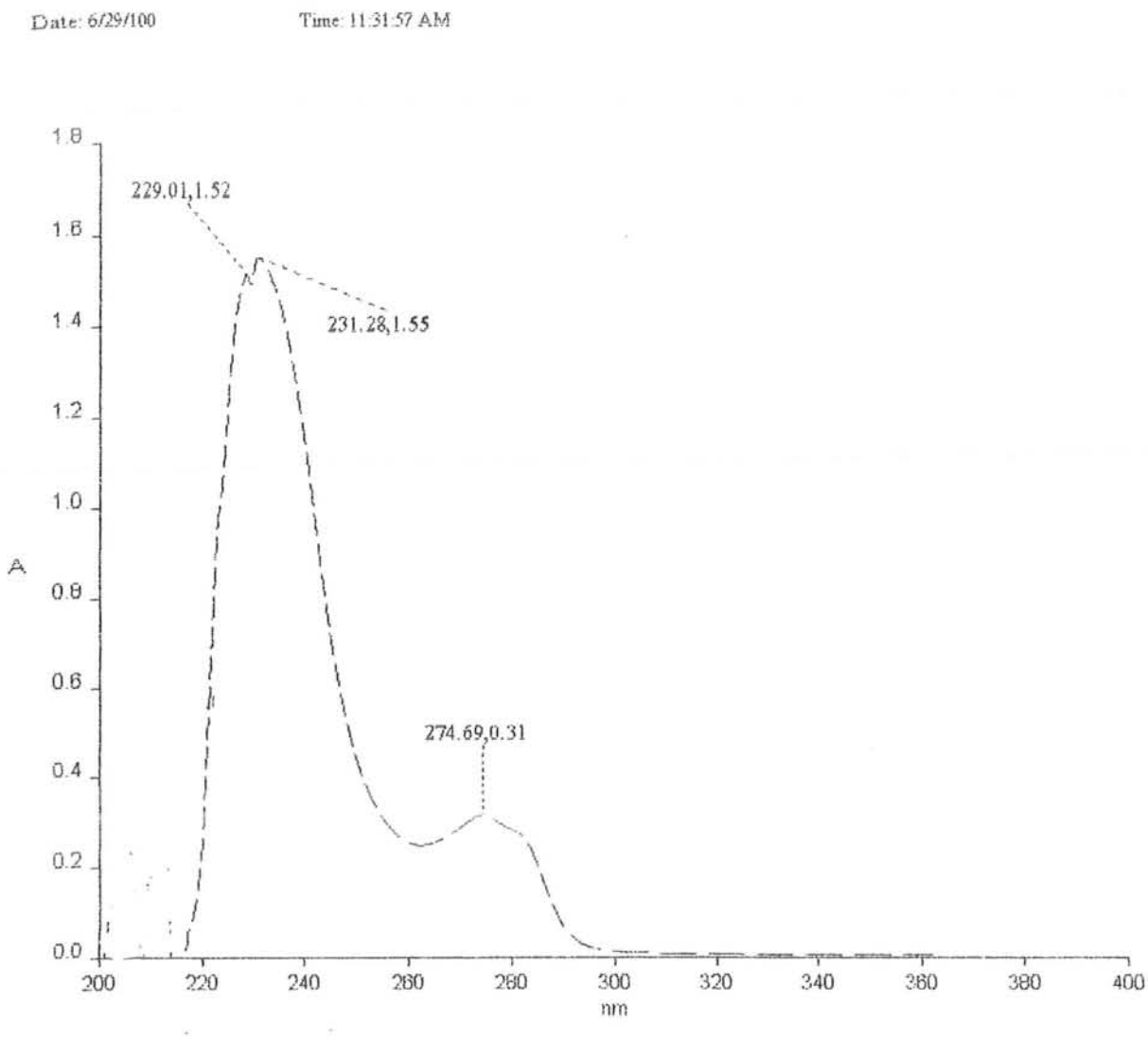

Fig.5.26 Absorption spectrum of exposed CR-39 from ^{241}Am, etched in 6M NaOH at 70 ^{o}C

5.5 CONCLUSIONS

1. Improved method for bulk etch rate determination gives better results than Henke Benton's method.

2. The systematic errors in V_B measurement can be minimize by imporved method.

3. The activation energy is independent to the nature of etchant.

4. KOH is more efficient for bulk etch rate than NaOH.

5. The before exposure absorbed water enhances the bulk etch rate of CR-39 .

6. The etchant concentration strongly effected on the alphas track diameters .

7. Bulk etch rate of CR-39 depends upon the absorbed dose of γ-rays.

8. It is found that the absorbance of UV light by CR-39 detectors dependence upon the exposure to the CR-39 detector as well as etching time.

References

REFERENCES

1. L. J. Malone (1994) Basic concepts of chemistry. (Fourth edition) John Wiley and Sons, New York, P.503.

2. G. F. Knoll (1989) Radiation detection and measurement (Second edition) John Wiley & Sons, New York, P.699.

3. D. A. Young (1958) Etching of radiation damage in lithium fluoride. Nature **182**, 375-377.

4. E. C. H. Silk and R. S. Barnes (1959) Examination of fission fragment tracks with an electron microscope. Phil. Mag. **4**, 970-972.

5. R. L. Fleischer, P. B. Price and R. M. Walker (1965) Solid-state track detectors: Applications to nuclear science and geophysics. Ann. Rev. Nucl. Sci. **15**, 1-28.

6. R. M. Walker, P. B. Price and Fleischer (1963) A versatile disposable dosimeter for slow and fast neutrons. Appl. Phys. Lett. **3**, 28-29.

7. R. L. Fleischer, P.B. Price and R. M. Walker (1965). The ion explosion spike mechanism for formation of charged particle tracks in solids. J. Appl. Physc. **36**, 3645-3652.

8. R. L. Fleischer et al. (1967) Criterion for registration in various solid state nuclear track detectors. Physc. Rev. **133**, 1443-1449.

9. P. B. Price et al. (1967) Identification of isotopes of energetic particles with dielectric track detectors. Phys. Rev. **164**, 1618-1620.

10. C. W. Naeser (1967) The use of apatite and sphene for fission track age determination. Bull. Geo. Soc. Am. **78**, 1523-1526.

11. K. Becker (1968) The effect of oxygen and humidity on charged particle registration in organic foil. Red. Res. **36**, 107-118.

12. W. G. Cross and L. Tommasino (1968) Electrical detection of fission fragment tracks for fast neutron dosimetry. Health Phys. **15**, 196.

13. P. B Price et al. (1968) Plastic track detectors for identifying cosmic rays. Can. J. Phys. **46**, 1149-1153.

14. D. Lal and R. S. Rajan (1969) Observation on space irradiation of individual crystals of gas-rich meteorites. Nature **223**, 269-271.

15. S. A. Durrani and R. H. Bull (1987) Solid state Nuclear Track Detection. Pergamon Press. Oxford.

16. G. Crozaz, R. Walker and D. Woolum (1971) Nuclear track studies of dynamic surface process on the moon and constancy of solar activity. Second Lunar Sci. Conf. Carbridge, Mass, 2543-2558.

17. R. L. Fleischer, P. B. Price and R. M. Walker (1975) Nuclear Tracks in Solids: Principle and Applications. University of California Press, Berkeley.

18. A. L. Frank and E. V. Benton (1975) Measurements with track-etch detector on working-level exposure in houses near uranium tailings. Dept. of Physics, University of San Francisco, Tech. Report 40.

19. A. Chambaudet, A. Bernas and J. Roncin (1977) On the formation of heavy ion latent tracks in polymeric detectors. Radiat. Effects. **34**, 57-59.

20. D. J. Gore, M. C. Thorne and R. H. Watts (1978) The visualization of fissionable-radionuclides in rat lung using neutron-induced autoradiography. Phys. Med. Biol. **23**, 149-153.

21. D. O'Sullivan, P. B. Price, K. Kinoshita and C. G. Willson (1982) Predicting radiation sensivity of polymers. J. Electrochem. Soc. **129**, 811-813.

22. B. G. Cartwright, E. K. Shirk and P. B. Price (1978) CR-39: a nuclear-track-recording polymer of unique sensitivity and resolution.Nucl.Instrum. Meth. **153**, 457-460.

23. R. M. Cassow and E. V. Benton (1978) Properties and applications of CR-39 polymeric nuclear track detector. Nucl. Track Detection **2**, 173-179.

24. M. Fujii and R. Yokota (1986) Thermosetting resins for nuclear track detection. Nuclear Tracks **12**, 55-58.

25. Data for CR-39 is collected from the information pages on CR-39 provided by Pershore Mouldings Limited.

26. L. t. Chadderton, S. A. Cruz and D. W. Find (1993) Theory for latent particle tracks in polymers. Nucl. Tracks Radiat. Meas. **22**, 29-38.

27. Robert Katz (1984) Formation of etchable tracks in plastics. Nucl. Tracks Radiat. Means. **8**, 1-8.

28. R. Katz and E. J. Kobetich (1968) Formation of etchable tracks in dielectrics. Phys. Rev. **170**, 401-405.

29. A. Sigrist and R. Balzer (1978) Investigations on the formation of tracks in crystals. Nucl. Track Detection **2**, 387--391.

30. M. Maurette (1970) Track formation mechanisms in minerals. Rad. Effects **3**, 149-154.

31. P. B. Price, R. L. Fleischer and C. D. Moak (1968) On the identification of very heavy cosmic ray tracks in meteorites. Phys. Rev. **167**, 277-282.

32. G. Somogyi (1984) Current problems in chemical track etching. Nucl. Tracks Radiat. Meas. **8**, 27-35.

33. A. Joseph and K. M. Varier (1995) A track development model for CR-39 for low energy alpha particles. Radiation Measurements **24**, 111-114.

34. H. A. Khan (1973) An important precaution in the etching of solid state nuclear track detectors. Nucl. Instrum. Meth. **109**, 515-519.

35. G. Somogyi (1977) Processing of plastic track detectors. Nucl. Track Detection **1**, 3-18.

36. S. K. Modgil and H. S. Virk (1984) Effect of etchant concentration and temperature on bulk etch rate for SSNTDs. Nucl. Tracks Radiat. Meas. **8**, 95-98.

37. P. H. Fowler and D. L. Henshaw (1978) Measurement of the cosmic ray elements. Nuclear Tracks. **2**, 1017-1021.

38. P. F. Green, A. G. Ramli, S. A. R. Al-Najjar, F. Abu-Jarad and S. A. Durrani (1982) A study of bulk-etch rates and track-etch rates in CR-39 Nucl. Instrum. Meth. **203**, 551-559.

39. R. Henke, K. Ogura and E. V. Benton (1986) Standard Method for measurement of bulk etch in CR-39. Nuclear Tracks **12**, 307-310.

40. E. V. Benton (1968) A study of charged particle tracks in cellulose nitrate. USNRDL-TR-68-14.

41. R. L. Fleischer and P. B. Price (1963) Tracks of charged particles in high polymers. Science **140**, 1221-1222.

42. G. Somogyi and I. Hunyadi (1979) Etching properties of the CR-39 polymeric nuclear track detector. Proc. 10th Int. Conf. SSNTD, Lyon, Pergamon Press, Oxford, PP, 443-452.

43. T. A. Gruhn, W. K. Li, E. V. Benton (1980) Etching mechanisms and behavior of polycarbonates in hydroxide solution: Lexan and CR-39. Nucl. Tracks. PP, 291-302.

44. J. Stejny, and T. Portwood (1986) A study of the molecular structure in CR-39. Nucl. Tracks **12**, 121-123.

45. R. L. Fleischer and P. B. Price (1963) Tracks of charged particles in high polymers. Science **140**, 1221-1222.

46. G. S. Randhawa, S. Kumar and H. S. Virk (1997) Response of different plastic track detectors to α-particles. Radiation Measurements **27**, 523-527.

47. B. Dorschel, R. Bretschneider and H. Kuhne (1999) Measurement of the track etch rates along proton and alpha particle trajectories in CR-39 and calculation of the detection efficiency. Radiation Measurements **31**, 103-108.

48. R. L. Fleischer and P. B. Price (1964) Glass dating by fission fragment tracks. J. Geophysics. Res. **69**, 331-339.

49. R. P. Henke and E. V. Benton (1971) on geometry of tracks in dielectric nuclear track detectors. Nucl. Instrum. Meth. **97**, 483-489.

50. Fleischer R. L., Price P. B. and Walker R. M. (1969) Nuclear tracks in solids. Scientific American **220**, 30-39.

51. P. A. Gottschalk, G. Grawert, P. Vater and R. Brandt (1983) Two-three-and four particle exit channels in the reaction (806 MeV) K_r + U Phys. Rev. **27**, 2703-2719.

52. P. A. Gottschalk, P.Valer , R.Brandt , I.E.Qureshi , H.A.Khan and G.Fiedler (1996) Kinematical analysis of heavy ion induced nuclear reactions using solid state nuclear track detectors, Physics of Particles and Nuclei **27(2)**, 154-178.

53. H. A. Khan and I. E. Qureshi (1999) SSNTD applications in science and technology. Radiation Measurements **31**, 25-36.

54. P. B. Price, J. D. Stevenson and H. L. Raven (1985) Discovery of radioactive decay of ^{222}Ra and ^{224}Ra by ^{14}C emission. Phys. Rev. Lett. **54**, 297-299.

55. I.E.Qureshi (1996) Heavy ion radioactivity. The Nucleus (Pakistan) **33(4)**, 31-42.

56. S. L. Guo and W. Huang (1997) Fission track dating of ancient man site Barise, China. Radiat Meas **28**, 565-570.

57. G.A. Wagner (1978) Archaeology applications of fission track dating Nucl. Tracks Det. **21**, 51-64.

58. R. L. Fleischer (1998) Tracks to Innovations: Nuclear Tracks in Science and Technology. Springer, New York.

59. A. A. Qureshi, M. A. Samad Beg and H. A. Khan (1988) Uranium exploration in Pakistan using alpha sensitive plastic films. Nucl. Track Radiat Meas. **15**, 735-739.

60. C. Y. King (1978) Radon emanation on San Andreas Fault. Nature **271**, 516-519.

61. S. A. Durrani (1993) Radon as a health hazard at home. What are the facts? Nucl Tracks Radiat Meas. **22**, 3030, 3037.

62. F. Spurny and K. Turek (1977) Neutron dosimetry and Solid State Nuclear Track Detectors. Nucl. Track Detection **1**, 189-197.

63. N. Ahmad, Matiullah and M. A. Kenawy (1997) A CR-39 based thermal neutron dosimeter. Radiation Measurements, **28**, 413-414.

64. R. Ilic (1990) The use of SSNTDs in materials science and technology, Nucl. Tracks Radiat. Meas. **17**, 7.

65. R. Brandt (1993) Some recent applied and fundamental work with SSNTD. Nucl. Tracks Radiat. Meas., **21**, 341-347.

66. R. M. Cassou and E. V. Benton. (1978) Properties and applications of CR-39 polymeric nuclear track detector. Nucl. Track detection, **2**, 173-179.

67. R. N. Mukherjee, P. K. Das. (1995) Particle identification by SSNTD-A new approach. Radiation Measurements, **24**, 67-73.

68. A. M. Marenny (1995) Two-decade experience of application of plastic detectors to cosmic ray research on satellites and orbital space stations. Radiation Meas. **25**, 315-323.

69. R. L. Fleischer and H. R. Hart, Jr (1973) Particle track record in Apollo 15 deep core from 54 to 80 cm depths. Sci. Lett. **18**, 420-426.

70. D. L. Henshaw, A. P. ews and D. J. Webster (1980) The microdistri-

bution of α-active nuclei in bronchial tissue by autoradiography using CR-39. Nucl. Tracks **4**, 649-654.

71. D. L. Henshaw and K. J. Heyward (1984) Comparison of the α-activity in the blood of smokers and non-smokers. Nucl. Tracks **8**, 453-456.

72. J. H. Fermlin and M. I. Edmonds (1980) The determination of lead in human teetch. Nucl. Instrum. Meth. **173**, 211-215.

73. T.Yamauchi, T. Taniguchi and S.Tagawa (1999) Dose- rate effects on the bulk etch rate of CR-39. Radiation Measurements **31** , 121-126 .